Dengue virus NS1 protein conveys pro-inflammatory signals by docking onto high-density lipoproteins

Souheyla Benfrid, Kyu-ho Park, Mariano Dellarole, James Voss, Carole Tamietti, Gérard Pehau-Arnaudet, Bertrand Raynal, Sébastien Brûlé, Patrick England, Xiaokang Zhang, et al.

Title: Dengue virus NS1 protein conveys pro-inflammatory signals by docking onto high-density lipoproteins

Authors: Souheyla Benfrid[1,2,#,*], Kyu-Ho Park[1,#,*], Mariano Dellarole[1,#], James E. Voss[1,#], Carole Tamietti[1], Gérard Pehau-Arnaudet[3], Bertrand Raynal[4], Sébastien Brûlé[4], Patrick England[4], Xiaokang Zhang[1,#], Anastassia Mikhailova[5,#], Milena Hasan[6], Marie-Noëlle Ungeheuer[7], Stéphane Petres[8], Scott B. Biering[9], Eva Harris[9], Anavaj Sakunthabaï[10], Philippe Buchy[11,#], Veasna Duong[11], Philippe Dussart[11], Fasséli Coulibaly[12], François Bontems[1,13], Félix A. Rey[1], Marie Flamand[1,†]

Affiliations:

[1]Unité de Virologie Structurale, Institut Pasteur and CNRS UMR3569, 25-28 rue du Docteur Roux, 75724 Paris, France

[2]Université Paris Descartes Sorbonne Paris Cité, France

[3]UTECH UBI, Institut Pasteur and CNRS UMR 3528, 28 rue du Docteur Roux, 75724 Paris, France

[4]Molecular Biophysics Facility, Institut Pasteur, CNRS UMR 3528, 25 rue du Docteur Roux, 75724 Paris, France

[5]HIV Inflammation et Persistance, Institut Pasteur, 28 rue du Docteur Roux, 75724 Paris, France

[6]Cytometry and Biomarkers Unit of Technology and Service, CB UTechS, 28 rue du Docteur Roux, 75724 Paris, France

[7]ICAReB, Institut Pasteur, 28 rue du Docteur Roux, 75724 Paris, France

[8]Production and Purification of Recombinant Proteins Facility, Institut Pasteur, 28 rue du Docteur Roux, 75724 Paris, France

[9]Division of Infectious Diseases and Vaccinology, School of Public Health, University of California, Berkeley, 185 Li Ka Shing Center, 1951 Oxford Street, Berkeley, CA, 94720-3370, USA

[10]Human Genetics, Institut Pasteur, 25 rue du Docteur Roux, 75724 Paris, France

[11]Virology Unit, Institut Pasteur du Cambodge, Institut Pasteur International Network, 5 Monivong Boulevard, PO Box 983, Phnom Penh, Cambodia

[12]Department of Biochemistry and Molecular Biology, Monash University, Clayton, 3800, Australia

[13]Département de Biologie et Chimie Structurales, Institut de Chimie des Substances Naturelles, CNRS UPR2301, Gif-sur-Yvette, France

[#]Present addresses: Université Paris-Est, Laboratoire de Santé Animale, ANSES, INRA, ENVA, UMR 1161 Virologie, 94700, Maisons-Alfort, France (SB); Applied Molecular Virology, Institut Pasteur Korea, Seongnam-si, Gyeonggi-do, Rep. of Korea (KHP); Virus Biophysics Laboratory, Bionanosciences Research Center (CIBION), National Scientific and Technical Research Council (CONICET), Godoy Cruz 2390, C1425FQD Ciudad Autónoma de Buenos Aires, Argentina (MD); Department of Immunology and Microbiology, The Scripps Research Institute, La Jolla, CA 92037, USA (JV); Guangdong Provincial Key Laboratory of Brain Connectome and Behavior, CAS Key Laboratory of Brain Connectome and Manipulation, the Brain Cognition and Brain Disease Institute (BCBDI), Shenzhen Institutes of Advanced Technology, Chinese Academy of Sciences; Shenzhen-Hong Kong Institute of Brain Science-Shenzhen Fundamental Research Institutions, Shenzhen, 518055, China (XZ); Division of Molecular Neurobiology, Department of Medical Biochemistry and Biophysics, Karolinska Institute, Stockholm, Sweden (AM); GlaxoSmithKline Vaccines R&D, Singapore (PB)

*These authors contributed equally to this work

[†]Correspondence to: Marie Flamand (marie.flamand@pasteur.fr)

Short title: NS1 forms a pro-inflammatory complex with HDL

Key words: Arbovirus, hemorrhagic fever, virulence factor, accessory protein, lipoprotein particle, molecular pathogenesis

ABSTRACT

The dengue virus nonstructural protein 1 (NS1) is a secreted virulence factor that modulates complement, activates immune cells and alters endothelial barriers. The molecular basis of these events remains incompletely understood. Here we describe a functional high affinity complex formed between NS1 and human high-density lipoproteins (HDL). Collapse of the soluble NS1 hexamer upon binding to the lipoprotein particle leads to the anchoring of amphipathic NS1 dimers into the HDL outer layer. The stable complex can be visualized by electron microscopy as a spherical HDL with rod-shaped NS1 dimers protruding from the surface. We further show that the assembly of NS1-HDL complexes triggers the production of pro-inflammatory cytokines in human primary macrophages while NS1 or HDL alone do not. Finally, we detect NS1 in complex with HDL and low-density lipoprotein (LDL) particles in the plasma of hospitalized dengue patients and observe NS1-apolipoprotein E-positive complexes accumulating overtime. The functional reprogramming of endogenous lipoprotein particles by NS1 as a means to exacerbate systemic inflammation during viral infection provides a new paradigm in dengue pathogenesis.

INTRODUCTION

Dengue virus (DENV) infects nearly 400 million people annually, leading to more than 500,000 hospitalizations (Bhatt *et al*, 2013; Wilder-Smith *et al*, 2019). The mortality rate varies from less than 1% to 10% depending on the epidemic and medical care provided to patients (« Dengue and Severe Dengue » s. d. WHO, 2016; (Yacoub *et al*, 2016)). The dengue nonstructural protein 1 (NS1) is a viral effector circulating in the bloodstream of DENV-infected patients (reviewed in (Glasner *et al*, 2018; Rastogi *et al*, 2016; Watterson *et al*, 2016)). In DENV-infected cells, NS1 forms amphipathic dimers in the endoplasmic reticulum (ER) that insert into the luminal side of the membrane (Akey *et al*, 2015; Lindenbach & Rice, 1997; Winkler *et al*, 1989). The membrane-bound dimers play an essential role in orchestrating viral replication in specialized subcellular factories (Lindenbach & Rice, 2003). A sub-fraction of NS1 dimers further associate by three to form barrel-shaped hexamers. During this process, NS1 hexamers detach from the ER membrane and are secreted as soluble nanoparticles loaded with lipids from the infected cell (Flamand *et al*, 1999; Gutsche *et al*, 2011). The secreted form of NS1 has previously been shown to bind to complement and coagulation factors, to activate immune and endothelial cells, to trigger the expression of pro-inflammatory cytokines, to alter the glycocalyx barrier and to promote endothelium permeability (Beatty *et al*, 2015; Flamand *et al*, 2009; Modhiran *et al*, 2017; Modhiran *et al*, 2015; Puerta-Guardo *et al*, 2019; Puerta-Guardo *et al*, 2016). The antibody response against NS1 has been shown to protect against several flavivirus infections (Beatty *et al.*, 2015; Brault *et al*, 2017; Espinosa *et al*, 2019; Schlesinger *et al*, 1985, 1987) but can also be harmful *via* a cross-reaction with platelets and endothelial cell surface antigens (Falconar, 2007; Jayathilaka *et al*, 2018; Lin *et al*, 2006; Lin *et al*, 2011; Sun *et al*, 2007; Wan *et al*, 2016). These characteristics altogether favor the development of thrombocytopenia, vascular leakage and hemorrhage. Given the growing evidence of NS1 involvement in dengue pathogenesis, a

94 better understanding of the molecular fate of NS1 in extracellular fluids by identifying its
95 interacting partners is of utmost importance.
96
97 In the present study, we report that NS1 from dengue virus serotype 2 (DENV-2) binds high-
98 density lipoproteins (HDL) and with a lower affinity low-density lipoproteins (LDL).
99 HDL and LDL are lipoprotein complexes composed of large lipid bundles surrounded by the
100 apolipoproteins A-I and B, respectively, as well as a panel of functional proteins recently
101 identified by proteomic approaches (Birner-Gruenberger *et al*, 2014; Ronsein & Vaisar,
102 2019). Lipoprotein particles that circulate in the blood have long been recognized for their
103 regulatory functions in vascular homeostasis, inflammation and innate immune responses
104 (Birner-Gruenberger *et al.*, 2014; Camont *et al*, 2011; Feingold & Grunfeld, 2000;
105 Ramasamy, 2014; Saemann *et al*, 2010). We explored the NS1-HDL association by
106 biophysical methods and visualized the complex by electron microscopy, which revealed NS1
107 dimers protruding on the HDL surface. We observed that the NS1-HDL complex could trigger
108 the production of pro-inflammatory cytokines in primary human macrophages. In addition,
109 we consistently detected elevated levels of NS1-HDL complexes in the blood of DENV-
110 infected patients on the day of hospital admission using an anti-apolipoprotein A-I (ApoA-I)
111 detection assay. NS1 complexes acquired an apolipoprotein E (ApoE)-positive phenotype
112 during the clinical phase, a component mostly found on very-low-density lipoproteins or
113 chylomicrons and only transiently associated with HDL or LDL in physiological conditions.
114 This points to a complex and dynamic interaction of DENV NS1 with the host lipoprotein
115 metabolic cycle.
116

RESULTS AND DISCUSSION

The DENV-2 NS1 hexamer binds high- and low-density lipoprotein particles

In this study, we first sought to identify NS1 protein partners encountered during its circulation in human blood. For this purpose, we carried out a pull-down assay using a purified preparation of recombinant streptavidin-tagged DENV2 NS1 spiked in plasma obtained from healthy donors to identify potential ligands. We then re-affinity purified NS1 from the plasma and analyzed the resulting products by size exclusion chromatography (SEC) (Fig. 1A). Compared to NS1 alone, the pull-down SEC profile showed an additional peak and a large shoulder at smaller elution volumes, corresponding to apparent molecular weights of 840 and 380 kDa, respectively (Fig. 1A). The protein content of the two high molecular weight complexes was analyzed by SDS-PAGE, and the identities of the predominant protein bands were determined by N-terminal sequencing and mass spectrometry as ApoA-I and ApoB. These proteins correspond to the main scaffold proteins of HDL and LDL, respectively (Fig. 1A). NS1-HDL and NS1-LDL complexes could also be detected in the extracellular media of S2 cells expressing recombinant NS1 and cultured in the presence of fetal bovine serum (FIG. EV1), as analyzed by size exclusion chromatography (Fig. EV1A), SDS-PAGE (Fig. EV1B) and negative stain electron microscopy (Fig. EV1C). As a matter of fact, in these experimental conditions NS1-ApoA-I and NS1-ApoB lipoprotein complexes were the predominant NS1 species and no significant level of free NS1 could be observed in the culture media (Fig. EV1A). Moreover, an association of native NS1 with a conformationally relevant ApoA-I could further be demonstrated by co-immunoprecipitation of DENV-infected cell culture supernatants supplemented with human serum using an anti-NS1 monoclonal antibody (MAb) or anti-ApoA-I polyclonal antibodies (PAb) (Fig. EV2A,B).

These observations prompted us to assess the affinity of DENV2 NS1 for HDL and LDL. We immobilized human HDL and LDL particles on bio-layer interferometry (BLI) sensors coated with specific polyclonal antibodies against ApoA-I or ApoB, respectively. Figure 1B displays the binding curves for increasing NS1 concentrations in contact with both types of lipoprotein particles and the values reached at steady state (also see Fig. EV3). The curves could be fitted using a single-state binding model, leading to relative binding constants (Kd) of 63 nM ± 0.2 nM and 1.4 μM ± 0.1 μM for HDL and LDL, respectively (Fig. 1B).

In order to characterize the architecture of the complex, we used analytical ultracentrifugation to study the behavior of NS1, HDL and a mix of HDL and NS1 at a HDL:hexameric NS1 molar ratio of 1:1 or 1:5 (Fig. 1C). Purified NS1 sedimented as a main species with a sedimentation coefficient of 7.9 S compatible with a globular hexamer. HDL particles exhibited a much lower value of 4.20 S in keeping with the larger lipid to protein ratio (Lauer *et al*, 2016). In the sample containing a 1:5 excess mass of NS1relative to HDL, all the HDL was engaged in an interaction with NS1. The unique species that was formed sedimented with a coefficient of 16.8 S, segregating distinctly from the other species (Fig. 1C). Residual unbound NS1 hexamer could still be observed, as expected due to the NS1 excess (Fig. 1C). By combining two detectors and taking into account the theoretical composition of the HDL particles, we estimated that one NS1 hexamer was bound to each HDL particle when present in excess. Interestingly, in the 1:1 ratio sample, we detected intermediate peaks at 9.4 and 11.7S that corresponded to one or two NS1 dimeric subunits bound to HDL, respectively.

The NS1 hexamer dissociates into discrete dimeric blocks on the surface of spherical HDL particles

Based on the above results, we prepared NS1-HDL complexes at a 1.5:1 NS1 to HDL molar ratio and examined the resulting products by negative-stain electron microscopy (EM). As previously shown, human HDL particles appeared as smooth spheres ~10 nm in diameter with an electron-dense central region (Zhang *et al*, 2013) (Fig. 2A). The purified NS1-HDL complexes, in contrast, presented a granular surface with prominent structures on their outer layer (Fig. 2B). 2D class averages of NS1-HDL complexes revealed that the HDL particles were crowned with high-density features that match very well with the contour of NS1 dimers in side view with two discrete nodules that likely correspond to the NS1 protomers (Fig. 2B, 2C) (Fig. EV4A,B) (Akey *et al.*, 2015; Lindenbach & Rice, 1997; Winkler *et al.*, 1989). Anti-NS1 Fabs confirmed the presence of NS1 dimers on the surface of HDL particles by forming salient outward projections (Fig. EV4C). Our analysis also revealed that about 60% of the NS1-HDL complexes presented three NS1 dimers on the HDL surface while around 25% and 10% of the particles presented 2 or 4 apparent NS1 dimers on their surface, respectively (Fig. 2B). These observations corroborated the ultracentrifugation data showing different ratios of NS1 dimers per HDL particle depending on the initial NS1:HDL ratio (Fig. 1C). This points to a dynamic binding mode between NS1 and HDL particles with, in particular, the collapse of NS1 hexamers into dimers upon binding to HDL particles as depicted in Fig. 2C.

The presence of NS1 dimeric subunits associated with HDL could also be evidenced by differential scanning calorimetry (DSC) (Fig. 2D). Thermal scanning of both hexameric NS1 and the NS1:HDL mixture (at a 1.5:1 molar ratio) showed two transition phases while the HDL particles alone did not contribute to any signal in the scanned temperature range (Fig. 2D) (Jayaraman *et al*, 2015). The second transition at a Tm of 81°C was identical for NS1 alone or in complex with HDL. We have previously reported that the NS1 dimer of

Japanese encephalitis virus requires temperatures higher than 80°C to dissociate into monomers (Flamand *et al*, 1995). We therefore attributed this second transition to the dissociation and full denaturation of NS1 dimeric subunits (Fig. 2D). Accordingly, the first transition peak corresponds to the dissociation of NS1 hexamers into dimers for NS1 alone (Tm of 59°C) and to the release of NS1 dimers from the HDL particle for the NS1-HDL mixture (Tm of 67°C) (Fig. 2D). The difference in Tm values observed for the first transition peak in both samples provides additional evidence that once the NS1-HDL complex formed, the NS1 dimer-dimer interface initially present in the hexamer is converted into a more stable interface formed between the NS1 dimers and the HDL surface.

We showed in a previous study that the NS1 dimeric building blocks behave as hydrophobic entities in a Triton X-114 phase partitioning assay (Gutsche *et al.*, 2011). Others reported that NS1 has the ability to interact with cellular membranes and liposomes (Akey *et al.*, 2015; Jacobs *et al*, 2000; Lindenbach & Rice, 1997; Winkler *et al.*, 1989). Thus, dimers have a propensity to interact with hydrophobic surfaces and lipids. The recent demonstration that NS1 binds ApoA-I through hydrophobic interactions (Coelho *et al*, 2021) suggests that this interaction may be important in promoting the collapse of the NS1 hexamer into dimers on the surface of the HDL particle. We were also able to show that the interaction between NS1 and HDL could be inhibited with anti-ApoA-I PAbs raising the question of the nature of the interaction between the NS1 hexamer and the ApoA-I protein at the initial stage of NS1 binding to HDL (Fig. 2E).

The NS1-HDL complex triggers pro-inflammatory signals in human primary macrophages

NS1 is known to trigger the production of pro-inflammatory cytokines in macrophages (Modhiran *et al.*, 2017). As NS1 associates to HDL, themselves potent modulators of inflammation (Camont *et al.*, 2011; Saemann *et al.*, 2010), we questioned the role of NS1 versus its complex NS1-HDL form in this process and characterized the cytokine and chemokine production pattern in human macrophages exposed to NS1 alone, HDL alone or to the NS1-HDL complex (Fig. 3). Primary macrophages were differentiated from isolated monocytes of various donors and stimulated with the different combinations of effectors. When exposed to NS1 or HDL alone, we observed no significant difference in the cytokine levels produced by macrophages compared to the negative control, whereas the bacterial lipopolysaccharide (LPS) consistently induced high levels of cytokine secretion (Fig. 3A-D). These observations ruled out any cytotoxic effect from putative contaminants in the NS1 and HDL samples. In contrast, the NS1-HDL mixture induced an increase in TNF-α (Fig. 3A), IL-6 (Fig. 3B), Il-1β (Fig. 3C) and IL-10 (Fig. 3D) secretion compared to NS1 alone. The differences were higher and all significant when compared with HDL alone, suggesting that NS1 converts HDL into pro-inflammatory signaling particles (Fig. 3A-D).

NS1-lipoprotein complexes are detected in hospitalized patients

Knowing that the concentration of the above-mentioned cytokines and chemokines is dramatically increased in patients with severe dengue (Fink *et al*, 2006; Green & Rothman, 2006; Pang *et al*, 2007; Yacoub *et al*, 2013), we assessed the presence of NS1-HDL and NS1-LDL complexes in DENV-infected patients. To this end, we developed different ELISA formats to detect and quantify NS1-lipoprotein complexes in human plasma in addition to NS1 itself (Fig. EV5A-D). We tested blood samples from dengue patients on their days of admission and discharge from hospital (Fig. 4A-E). This represented on average a time interval of 4.3 days between the first and last samples. The vast majority of patients

(around 80%) showed significantly elevated NS1 and NS1-HDL, indicated by NS1-ApoA-I signals, in blood on the day of admission compared to the last sample (Fig. 4B,C). The highest concentrations were observed between day 2 and day 4 post-onset of fever and the signal waned to background levels by day 9. Over this period of time, levels of NS1-LDL complexes remained relatively low (Fig. 4E), despite the fact that 69% of the samples tested were positive. The size of the scaffold apolipoprotein B (ApoB, over 500 kDa) could not account for an accessibility issue of the protein to the detection antibodies, as opposed to ApoA-I of 25 kDa in size. This difference likely resulted from a lower affinity of NS1 for LDL relative to HDL, as suggested by our *in vitro* observations (Fig. 1B), or to a lower concentration of LDL in DENV-infected individuals compared to HDL. Apolipoprotein E (ApoE), which associated to native NS1 in DENV-infected cell supernatants (Fig. EV2B), appeared as another marker of NS1-lipoprotein complexes. As opposed to the NS1-ApoA-I trend, NS1-ApoE concentrations increased over time and were the highest when tested on blood specimens recovered at the time of patient discharge from hospital (Fig. 4D). Interestingly, important changes in lipid concentrations could be observed over the same period of time with a transient drop in cholesterol and a concomitant rise in triglyceride (Fig. 4F-H). These findings raise the question as to whether the DENV NS1 protein accounts for these fluctuations and to which extent the viral protein impacts host lipid and lipoprotein metabolic pathways. This concern extends to other flaviruses as well as we found that different flavivirus NS1 proteins have the ability to associate to HDL particles (Fig. 4I).

Dengue virus NS1 is a viral virulence factor that contributes to the development of severe dengue, characterized by cytokine storm, thrombocytopenia, vascular leakage and hemorrhage (Akey *et al.*, 2015; Glasner *et al.*, 2018; Rastogi *et al.*, 2016; Watterson *et al.*,

2016). NS1 circulates in the blood of DENV-infected patients at nanogram to microgram per ml levels (Alcon-LePoder *et al*, 2006; Antunes *et al*, 2015; Libraty *et al*, 2002). NS1 can trigger the production of inflammatory cytokines and chemokines in cell culture and in immunodeficient mice (Alayli & Scholle, 2016; Beatty *et al.*, 2015; Chen *et al*, 2015; Modhiran *et al.*, 2015). Our findings demonstrate that the formation of NS1-HDL complexes is a prerequisite for this effector function. The association of NS1 and HDL triggers pro-inflammatory signals in primary human macrophages while NS1 or HDL alone have no comparable effect. Also, an interaction of NS1 with a lipid-free ApoA-I purified from inclusion bodies and refolded *in vitro* generates inactive complexes (Coelho *et al.*, 2021). It has long been recognized that mature HDL particles, in which the scaffold ApoA-I protein interacts with specific classes of lipids and accessory proteins (Gogonea, 2015), have an anti-inflammatory regulatory function and contribute to the maintenance of vascular integrity under physiological conditions (Birner-Gruenberger *et al.*, 2014; Camont *et al.*, 2011; Ramasamy, 2014; Saemann *et al.*, 2010). However, the recruitment of certain proteins by HDL, such as serum amyloid A (SAA), confers a pro-inflammatory status to these particles during an acute phase response (Kopecky *et al*, 2017; Marsche *et al*, 2013; Murch *et al*, 2007; Prufer *et al*, 2015; Wu *et al*, 2004). Our working hypothesis is that NS1 exerts a similar control on HDL during DENV infections. This process could involve the HDL scavenger receptor B1 that has recently been identified as a cell surface receptor for DENV NS1 (Alcala *et al*, 2022), allowing its internalization in many mammalian cell types including macrophages, endothelial cells, keratinocytes and hepatocytes. An NS1-HDL contribution to the cytokine storm would have a direct impact on the development of severe dengue, as increased levels of TNFα, IL6 and IL-10 correlate consistently with disease severity and in certain instances endothelium permeability (Abhishek *et al*, 2017; Dewi *et al*, 2004; Huang

287 *et al*, 2018; Lee *et al*, 2016; Rathakrishnan *et al*, 2012; Srikiatkhachorn *et al*, 2017;
288 Tramontini Gomes de Sousa Cardozo *et al*, 2017).
289
290 Several studies have described altered levels of HDL, LDL or VLDL in severe dengue
291 (Barrientos-Arenas *et al*, 2018; Biswas *et al*, 2015; Lima *et al*, 2019; Marin-Palma *et al*, 2019;
292 Suvarna & Rane, 2009; van Gorp *et al*, 2002). It is conceivable that NS1 broadly impacts the
293 lipoprotein network by modifying the signaling patterns associated to the different lipoprotein
294 particles or modulating their metabolic turnover. In this respect, we report a dynamic
295 interaction of NS1 with host lipoproteins illustrated by a predominant binding to ApoA-I and
296 ApoB-positive lipoprotein complexes, representative of HDL and LDL species, and the
297 acquisition of an ApoE-positive signature over the course of the disease. ApoE is an
298 exchangeable lipoprotein that can associate with most lipoprotein particles during the lipid
299 metabolic cycle (Marais, 2019; Su & Peng, 2020). ApoE has also been recognized for its anti-
300 inflammatory, anti-oxidative, anti-thrombotic and endothelial repair related properties (Filou
301 *et al*, 2016; Valanti *et al*, 2018). Further studies are now needed to investigate whether the
302 formation of NS1-ApoE-positive lipoprotein complexes is part of a recovery mechanism from
303 the host or whether NS1 continues its pathogenic reprogramming during the convalescent
304 phase by interfering with ApoE function. A number of studies have described a persistence
305 of asthenia for weeks in dengue patients, extending well beyond the end of the acute clinical
306 phase (Halsey *et al*, 2014; Luengas *et al*, 2015; Teixeira *et al*, 2017; Tiga-Loza *et al*, 2020).
307
308 We previously described that NS1 is secreted from DENV-infected cells as an atypical
309 lipoprotein hexamer (Gutsche *et al.*, 2011). Once bound to an HDL particle, the NS1 hexamer
310 appears to collapse into its dimeric building blocks that eventually stick to the surface of the
311 lipoprotein particle. It is not clear at this stage to which extent protein-lipid or protein-protein

interactions prevail but both are likely to be important. Indeed, NS1 dimers are known to have the ability to bind lipid membranes, liposomes and separate in detergent phases [7-9] and all the candidate NS1 protein ligands published so far belong to the HDL proteome (Avirutnan *et al*, 2006; Chung *et al*, 2006; Coelho *et al.*, 2021; Conde *et al*, 2016; Kurosu *et al*, 2007; Lin *et al*, 2012; Shao & Heinecke, 2018). These proteins include the scaffold protein ApoA-I, complement factors C4, C1s, hnRNP C1/C2, factor H, prothrombin, as well as inhibitory factors of complement clusterin, C5-9 and SC5b-9 complexes (Avirutnan *et al.*, 2006; Chung *et al.*, 2006; Coelho *et al.*, 2021; Conde *et al.*, 2016; Kurosu *et al.*, 2007; Lin *et al.*, 2012). The interaction between NS1 and ApoA-I is reported to involve hydrophobic interactions (Coelho *et al.*, 2021), suggesting that once the NS1 hexamer binds the HDL particle, an interaction between NS1 and ApoA-I could trigger the dissociation of the NS1 hexamer in favor of a more stable dimer-ApoA-I interface. This is corroborated by our finding that the NS1 dimeric subunits have a higher thermal requirement to dissociate from the HDL particle than from the NS1 hexamer itself (Fig. 2D). It should be noted though that the docking of NS1 to HDL particles may involve other binding determinants than ApoA-I, as NS1 also binds to LDL in which ApoA-I is poorly represented. Proteomic studies, direct protein-protein interaction assays or the use of synthetic lipoprotein particles with defined compositions will be instrumental in delineating the role of the different NS1 partners in the formation of biologically relevant NS1-lipoprotein complexes.

In conclusion, we provide evidence of a direct binding of NS1 to the surface of spherical HDL particles and to a lesser extent LDL particles as well. Once bound to HDL, NS1 undergoes a structural transition that results in the dissociation of NS1 hexamers and the anchoring of its amphipathic dimeric subunits onto the HDL surface. The association of NS1 and HDL triggers pro-inflammatory signals in primary macrophages, as a possible means to increase

vascular permeability and virus propagation in the infected organism. We further show that NS1-HDL concentrations are the highest at the time patients are admitted at hospital and by the end of the hospitalization period, NS1 complexes acquire an ApoE-positive signature the function of which remains to be explored. Other biological questions that need to be addressed relate to the molecular determinants of NS1 binding to various types of lipoprotein species, the receptors engaged by NS1-lipoprotein complexes during host cell interactions, their respective contribution to signal transduction and the role of proteins and lipids in the overall dynamics of the system. Unraveling the molecular mechanisms governing the assembly of the NS1-HDL complex, its metabolic fate and pathogenic functions will be critical in defining preventive measures against dengue and possibly other flaviviroses of public health concern.

MATERIALS AND METHODS

Cell line and viral infection

Vero cells (ATCC CRL-1586) were grown at 37°C with 5% CO_2 in DMEM (Gibco) supplemented with 10% fetal calf serum (Gibco) and 1% penicillin/streptomycinin. Vero cells were tested negative in mycoplasma with the MycoAlert Mycoplasma Detection kit (Lonza, LT07-318). Vero cells wee infected with DENV type 2 (strain 16681) at a multiplicity of infection of 1 and incubated for 3 days at 37°C with 5% CO_2.

DENV-2 NS1 protein expression, purification and serum pull-down experiments

The DENV-2 recombinant NS1 protein was expressed in Drosophila S2 cells and purified from the extracellular medium as detailed in the previously published supplementary methods (Gutsche *et al.*, 2011). Purified DENV-2 recombinant NS1 protein was incubated for 1h at 37°C in serum or plasma recovered from a healthy donor (provided by the ICAReB facility, Institut Pasteur) at a final concentration of 400 µg NS1/mL plasma. The mix was then purified on a Strep-tactin column (Iba), washed twice with PBS Mg^{2+}/Ca^{2+} (Gibco) followed by 14 column volumes of PBS 0.3 M NaCl and another 5 column volumes of PBS Mg^{2+}/Ca^{2+}. Elution was performed using 2.5 mM D-desthobiotine (Iba) in PBS Mg^{2+}/Ca^{2+}.

Purified samples of recombinant NS1, human HDL (Merck Millipore), human LDLs (Merck Millipore) or an *in vitro* reconstituted NS1-HDL mix were analyzed by size exclusion chromatography on a Superdex 200 10/300 column (GE healthcare). Protein standards from Bio-Rad were used to interpret elution profiles. The protein samples from the major peaks were further denatured in 5x Laemmli sample buffer containing β-mercaptoethanol, boiled for 5 min at 95°C and separated by discontinuous sodium dodecyl sulfate (SDS) 4-15%

372 polyacrylamide gel electrophoresis (SDS-PAGE precast gels, Bio-Rad). The SDS-PAGE gels
373 were stained in Coomassie Blue solution (Bio-Rad).
374
375 **Biolayer Interferometry**
376 DENV2 NS1 binding to HDL and LDL particles was monitored by Biolayer Interferometry
377 (BLI), using an Octet Red384 instrument (ForteBio). Streptavidin-coated biosensors (SA,
378 ForteBio) were loaded with biotinylated anti-ApoA-I or anti Apo-B antibodies (Abcam),
379 followed by HDL or LDL, respectively. Subsequently the biosensors were incubated in wells
380 containing serial dilutions of NS1 protein (concentrations ranging from 6.25 to 800nM for
381 HDL, and from 36 to 2500nM for LDL) and the BLI association signals were recorded in
382 real-time until they reached a plateau. Finally, the biosensors were incubated in wells
383 containing buffer to monitor the dissociation of the complexes formed, before being
384 regenerated for further use in replicate experiments. The regeneration protocol, comprising
385 three subsequent 20 seconds washes in 10 mM Gly-HCl pH2, could be applied up to eight
386 times for up to two days without losing any loading capacity of the immobilized biotinylated
387 antibodies. The specific NS1 binding curves were obtained by subtracting the non-specific
388 signals measured on unloaded biosensors used as control references. The steady-state signals
389 were determined at the end of the association step and fitted using the following equation:
390 Req= Rmax*C/Kd+C where Req is the steady-state BLI response, C the NS1 concentration,
391 and Rmax the response at infinite concentration. All measurements were performed at least
392 three times to determine experimental error. All experiments were performed at 20°C in PBS
393 Mg^{2+}/Ca^{2+} (Gibco) supplemented with 0.1% milk to minimize nonspecific binding, using 96-
394 well half-area plates (Greiner Bio6One) filled with 150 µl per well, and a shaking speed of

1000 rpm. Data was processed using the Scrubber (v2.0 BioLogic), BIAevaluation 4.0 (Biacore) and Profit (Quantumsoft) softwares.

Binding inhibition of NS1 to HDL with anti-ApoA-I antibodies was assessed using streptavidin-coated SA sensors (ForteBio) coated for 900s with biotinylated anti-ApoA-I polyclonal antibodies (Abcam, 5µg/ml in PBS-milk). Sensors were then further loaded for 900s with purified HDL (Cell Biolabs, 20µg/ml). Half of the HDL-loaded sensors were then saturated with anti-ApoA-I antibodies (5µg/ml for 900s), while the other half were just washed with buffer. Finally, all sensors were incubated into an NS1 solution (200nM) for 1200s, and the levels of NS1 binding recorded as described above.

Analytical ultracentrifugation

NS1, HDL, and NS1-HDL mixtures at different molar ratios were incubated 1h at 37°C and centrifuged at 32,000 rpm for the complexes in a XL-I and an Optima AUC (Beckman Coulter) analytical ultracentrifuge, at 20°C in a four-hole AN 50-Ti rotor equipped with 3-mm and 12-mm double-sector aluminum epoxy centrepieces.

Detection of the biomolecule concentration as a function of radial position and time was performed by absorbance measurements at 250 nm and 280 nm and by interference detection. Ultracentrifugation experiments were performed in PBS+/+ (Gibco). Extinction coefficients were extrapolated at 250 nm using the Utrascan II software. Sedimentation velocity data analysis was performed by continuous size distribution analysis c(s) using the Sedfit 15.0 software (Brown & Schuck, 2006). All the c(s) distributions were calculated with a fitted fractional ratio f/f0 and a maximum entropy regularization procedure with a confidence level of 0.95. Buffer viscosity and density as well as the extinction coefficient of NS1 were calculated using the sednterp software (http://www.jphilo.mailway.com/download.htm).

Molecular Mass and partial specific volume of NS1 and HDL were calculated from multidetection AUC experiment. NS1 have estimated mass for the monomer of 43 kDa with a partial specific volume of 0.721. HDL have estimated mass of 164 kDa, in agreement with mass photometry measurement (162 kDa, Fig. EV5F), and a partial specific volume of 0.843 ml.g-1 in agreement with the estimation from CsCl gradient (0.850 ml.g-1). Deconvolution of the multi-detector signal into stoichiometric ratio was performed by integrating all the peaks on each detector to determine the contribution of each partner present (NS1, HDL or both) and solving the contribution of each partner to the signal.

Taking these measurements into consideration, we can convert a mass ratio to a molar ratio as follows: a NS1:HDL mass ratio of 1:1 corresponds to a 1:1.6 molar ratio.

Differential scanning calorimetry (DSC)

Thermal unfolding of NS1 and of the NS1-HDL complex were followed using a VP-Capillary DSC instrument (Malvern MicroCal) in PBS buffer. The concentration of the NS1 hexamer was 0.2 mg/ml and was used at a 2:1 molar ratio to form the NS1-HDL complex. At least two DSC scans were recorded for each sample. Human HDL (Merck Millipore) was incubated with NS1 for 1 h at 37ºC prior to the DSC experiments. Scan rate was 100ºC/h with a filtering period of 2. Thermograms were analyzed with the Origin software provided by the manufacturer.

Electron microscopy and image analysis

Solutions of NS1 and NS1-HDL were spotted on glow-discharged carbon grids, contrasted with 2% uranyl acetate and imaged with a Tecnai F20 microscope (Thermo Fisher, USA) in low-dose conditions. Automated acquisitions were performed using EPU software (Thermo

Fisher, USA) and images were acquired using a Falcon II (Thermo Fisher, USA) direct detector.

HDL and NS1-HDL images were CTF-corrected (phase flip) and sorted using the XMIP software (Velazquez-Muriel *et al*, 2005). Corrected images were imported in Relion (Scheres, 2012). The recommended strategy for particle picking was applied as follow: a manual selection of particles compatible with the HDL or NS1-HDL size was performed on a small number (about fifteen) of images. A 2D classification (40 classes) was performed, and five representative well-defined classes were selected as template for the automatic picking, leading to about 30,000 particles. A 2D classification (200 classes) was then performed. Classes obviously corresponding to artefacts were suppressed and a final run of 2D classification (200 classes) was carried out.

Capture ELISA of NS1-lipoprotein complexes

Microtitration plates were coated overnight with purified mouse anti-NS1 monoclonal antibody (MAb DEN-2 17A12). Wells were saturated and washed before serial dilutions of human sera spiked with purified DENV-2 NS1 or DENV1- or DENV-2-infected human sera were added to wells for 2 h at room temperature. Wells were washed again and incubated for 1 h at 37°C with anti-ApoA-I (Novus Biologicals), ApoB or ApoE (Merck Chemicals LTD) polyclonal antibodies followed by a peroxidase-conjugated secondary antibody (Jackson ImmunoResearch Laboratories) detected with a 3,3", 5,5"-tetramethyl-benzidine solution (UltraTMB, ThermoFischer). Negative controls were measured when the reaction was carried out in the absence of antigen. Absorbance values were corrected by subtracting the mean value of the signal measured for the negative controls.

Flavivirus NS1 proteins binding to HDL in human plasma

Purified NS1 from different flaviviruses (yellow fever, YF; ZIKA; West Nile, WN; Japanese encephalitis, JE; The Native Antigen Company) were spiked for 1h30 at 37°C in normal human plasma and NS1-HDL complexes were further detected by the NS1-ApoA-I complex-specific ELISA (see Fig. EV5C). Flavivirus NS1-ApoA-I complexes were captured using an immobilized anti-dengue NS1 MAb cross-reactive for flavivirus NS1 protein. Bound ApoA-I was further detected using a specific goat polyclonal antibody (Novus Biologicals) followed by a species-specific peroxidase-labeled secondary antibody (Jackson ImmunoResearch Laboratories). The concentration values reported on the x-axis are given as an NS1 equivalent concentration.

Macrophages immune activation assay

Human monocytes were isolated from buffy coats and differentiated into macrophages in medium supplemented with human AB serum, as previously described (Allouch *et al*, 2013). Briefly, PBMCs were isolated from whole blood using a Ficoll gradient centrifugation (Eurobio). $CD14^+$ cells were purified by magnetic bead separation of PBMCs using $CD14^+$ human positive selection kit (StemCell) and plated $1x10^6$ cells/mL on Teflon plates (Sarstedt) with 7 ml per plate in the following medium: RPMI-1640 (Gibco), 2 mM L-glutamine (LifeTechnologies), 1% penicillin-streptomycin (10,000 units penicillin and 10 mg streptomycin/mL; Life Tech), 10 mM Na Pyruvate (Life Tech), 10 mM HEPES (Life Tech), 1% MEM vitamins (Life Tech), 1% NEAA (Life Tech), 50 uM beta-mercaptoethanol (Life Tech), and 15% human serum (ICAReB facility, Institut Pasteur). Monocytes were cultured in differentiating medium for 6-8 days, after which the macrophages were scraped off Teflon

plates and counted. After spinning, the cells were resuspended at $1x10^6$/mL in the same medium but with 5% FBS instead of human serum.

Macrophages were plated at 0.5 million cells per mL in P24 plates (Corning) and left 2 h in the incubator for cell sedimentation. Aliquotes of serum-free media (Optipro, Gibco) were supplemented with NS1 (10 µg/mL), HDL (2.5 µg/mL), a NS1-HDL mix at the same respective quantities (2.5 NS1:1 HDL molar ratio), an equivalent volume of PBS as negative control, LPS (100 ng/mL) as positive control, and incubated for 1h at 37°C. Macrophages were then exposed to the different suspensions for 24h before collecting supernatants. Inflammatory mediators were detected in clarified cell supernatants using a hMagnetic Luminex Assay 5 Plex, R&D Systems, Bio-Techne Ltd run on the BioPlex 200 System xMAP (BioRad Laboratories Inc.) as per the manufacturer's specifications. The antibody bead kit was designed to quantify IL-1β, IL-6, IL-10, TNF-α. Standards were run with each plate at every assay to titrate the level of cytokines present. Statistical analyses were performed in Prism 6.0 (GraphPad Software Inc.) Data are shown as individual points and means ± SD. Significant testing was performed using 2-way ANOVA.

DENV-infected patient sera

Patients presenting acute dengue-like symptoms – between June and October of 2011 and 2012 – were enrolled at the Kampong Cham Referral Hospital, Cambodia. Inclusion criteria, following the WHO 1997 classification scheme, were children between 2 and 15 years old who had fever or history of fever at presentation and onset of at least two of the following symptoms within the previous 72 hours: headache, retro-orbital pain, muscle pain, joint pain, rash, or any bleeding signs. We performed a prospective, monocentric, cross-sectional study of hospitalized children with severe and non-severe dengue. The study was approved by the

Cambodian National Ethics Committee for Human Research (approval #087NECHR/2011). All patient enrollment and blood sampling occurred after obtaining written informed consent from the patient's parents or guardians. The first visit was conducted at hospital admission. The day of onset of symptoms was defined as day 0 of the illness. The last visit was performed at the time of discharge for patients who recovered entirely, or as a follow-up visit for patients still in the critical phase. A clinical and biological follow-up including abdominal/chest ultrasound recording was conducted at each visit. DENV infection of hospitalized patients was confirmed by NS1 antigen detection using NS1-capture ELISA (Alcon-LePoder *et al.*, 2006; Antunes *et al.*, 2015; Libraty *et al.*, 2002) and/or RT-qPCR and/or virus isolation on *Aedes albopictus* C6/36 cells on the plasma sample obtained at admission (Andries *et al*, 2015). We observed that the NS1-capture ELISA set-up based on the NS1 capture with the 4F7 MAb and the NS1 antigen detection with a peroxidase-labeled 8G6 MAb could efficiently detect the soluble NS1 hexamer or NS1 dimers associated to HDL but not the NS1 protein interacting with ApoE.

Biosafety

Dengue virus-infected plasma samples were handled in a dedicated biosafety level (BSL)-3 laboratory. The biosafety manual describes standard and specific operating procedures. It is elaborated with the support of our institution and adopted by all BSL3 users.

DATA AVAILABILITY

No large primary datasets have been generated and deposited.

ACKNOWLEDGMENTS

The authors gratefully acknowledge the staff of the Kampong Cham Referral Hospital, the patients and parents who participated in the study, and the Arbovirus Team in the Virology Unit at the Institut Pasteur du Cambodge who contributed to this study. We acknowledge the participation of the ICAReB facility in setting up the recruitment of donors and the acquisition of blood samples, in particular Gloria Morizot, Bianca Liliana Perlaza, Sophie Chaouche, Linda Sangari, Céline Chapel, Philippe Esterre and Hélène Laude. We are most grateful to Christine Girard-Blanc and Evelyne Dufour for their contribution in producing and purifying the recombinant DENV NS1 protein, to Béatrice Poirier-Beaudouin and Cartini Mardi for their help in setting up the cytokine quantification assay, to Arvind Sharma for providing purified anti-E MAbs and to Mathilde Ban for preparing Fab-bound NS1-HDL complexes. We thank M. Nilges and the Equipex CACSICE for providing the Falcon II direct detector and David Veesler for his help in acquiring the first electron microscopy images of the bovine NS1-HDL complex. Finally, we thank Alexandre Pachot and Karine Kaiser for their support at the early stage of the project.

This study benefited from the financial support of the Institut Pasteur ACIP-27-16 (P.D., V.D., M.F.); the Institut Pasteur Dengue Task Force (to MF); the Institut Pasteur INNOV-44-19 (M.F); the National Natural Science Foundation of China 31600606 (X.Z.); the National Key R&D Program of China 2016YFA0501100 (X.Z.); Guangdong Provincial Key Laboratory of Brain Connectome and Behavior 2017B030301017 (X.Z.); CAS Key Laboratory of Brain Connectome and Manipulation 2019DP173024 (X.Z.); the NIAID/NIH

559 R01 AI24493 (E.H.) and R21 AI146464 (E.H.); Equipex CACSICE ANR-11-EQPX-0008
560 (G.P.-A.).

561

562 **DISCLOSURE AND COMPETING INTERESTS STATEMENT**

563 Dr. Philippe Buchy is a former Head of Virology at Institut Pasteur du Cambodge and is
564 currently an employee of GSK Vaccines, Singapore.

565 Part of the work is patented (PCT/EP2020/07714).

566

567 **AUTHORS CONTRIBUTION**

568 SB, K-HP, MD, FC, FB, FR and MF conceived and designed the experiments. SB, K-HP,
569 MD, JEV, CT, GP-A, BR, SB, PE, XZ, AM, MH, SP, SBB, FC, FB, MF performed the
570 experiments. SB, K-HP, JEV, CT, SP and FC expressed and purified the NS1 protein and its
571 complexes. SB, K-HP, MD, BR, SB and PE carried out the biophysical characterization of
572 protein complexes. GP-A, XZ and FB collected and processed the EM data and built the
573 model of the NS1-HDL complex. K-HP, CT, M-NU, MH and MF elaborated and developed
574 the different quantification assays formats. K-HP, CT, AS, PB, VD, PD and MF recruited the
575 dengue patient and tested the biological samples. SB, K-HP, MD, EH, FC, FB, FR and MF
576 wrote the manuscript. All authors discussed the experiments and approved the manuscript.

577

578 **ETHICS STATEMENT**

579 The study on dengue virus-infected patients was approved by the Cambodian National Ethics
580 Committee for Human Research (approval #087NECHR/2011). All patient inclusion and
581 blood sampling occurred after obtaining written informed consent from the patient's parents
582 or guardians.

583 Primary monocyte-derived macrophages were isolated from healthy donor blood obtained
584 from the French blood bank (Etablissement Français du Sang) as part of a convention with
585 the Institut Pasteur. In accordance with French law, written informed consent to use the cells
586 for clinical research was obtained from each donor.

REFERENCES

Abhishek KS, Chakravarti A, Baveja CP, Kumar N, Siddiqui O, Kumar S (2017) Association of interleukin-2, -4 and -10 with dengue severity. *Indian J Pathol Microbiol* 60: 66-69

Akey DL, Brown WC, Jose J, Kuhn RJ, Smith JL (2015) Structure-guided insights on the role of NS1 in flavivirus infection. *Bioessays* 37: 489-494

Alayli F, Scholle F (2016) Dengue virus NS1 enhances viral replication and pro-inflammatory cytokine production in human dendritic cells. *Virology* 496: 227-236

Alcala AC, Maravillas JL, Meza D, Ramirez OT, Ludert JE, Palomares LA (2022) The dengue virus non-structural protein 1 (NS1) uses the scavenger receptor B1 as a cell receptor in cultured cells. *J Virol*: JVI0166421

Alcon-LePoder S, Sivard P, Drouet MT, Talarmin A, Rice C, Flamand M (2006) Secretion of flaviviral non-structural protein NS1: from diagnosis to pathogenesis. *Novartis Foundation symposium* 277: 233-247; discussion 247-253

Allouch A, David A, Amie SM, Lahouassa H, Chartier L, Margottin-Goguet F, Barre-Sinoussi F, Kim B, Saez-Cirion A, Pancino G (2013) p21-mediated RNR2 repression restricts HIV-1 replication in macrophages by inhibiting dNTP biosynthesis pathway. *Proc Natl Acad Sci U S A* 110: E3997-4006

Andries AC, Duong V, Ly S, Cappelle J, Kim KS, Lorn Try P, Ros S, Ong S, Huy R, Horwood P *et al* (2015) Value of Routine Dengue Diagnostic Tests in Urine and Saliva Specimens. *PLoS neglected tropical diseases* 9: e0004100

Antunes P, Watterson D, Parmvi M, Burger R, Boisen A, Young P, Cooper MA, Hansen MF, Ranzoni A, Donolato M (2015) Quantification of NS1 dengue biomarker in serum via optomagnetic nanocluster detection. *Sci Rep* 5: 16145

Avirutnan P, Punyadee N, Noisakran S, Komoltri C, Thiemmeca S, Auethavornanan K, Jairungsri A, Kanlaya R, Tangthawornchaikul N, Puttikhunt C *et al* (2006) Vascular leakage in severe dengue virus infections: a potential role for the nonstructural viral protein NS1 and complement. *J Infect Dis* 193: 1078-1088

Barrientos-Arenas E, Henao-Garcia V, Giraldo DM, Cardona MM, Urcuqui-Inchima S, Castano JC, Hernandez JC (2018) [Modulation of high-density lipoprotein and cytokine IL-1beta and IL-6 levels in patients with dengue]. *Rev Peru Med Exp Salud Publica* 35: 15-24

Beatty PR, Puerta-Guardo H, Killingbeck SS, Glasner DR, Hopkins K, Harris E (2015) Dengue virus NS1 triggers endothelial permeability and vascular leak that is prevented by NS1 vaccination. *Sci Transl Med* 7: 304ra141

Bhatt S, Gething PW, Brady OJ, Messina JP, Farlow AW, Moyes CL, Drake JM, Brownstein JS, Hoen AG, Sankoh O *et al* (2013) The global distribution and burden of dengue. *Nature* 496: 504-507

Birner-Gruenberger R, Schittmayer M, Holzer M, Marsche G (2014) Understanding high-density lipoprotein function in disease: recent advances in proteomics unravel the complexity of its composition and biology. *Progress in lipid research* 56: 36-46

Biswas HH, Gordon A, Nunez A, Perez MA, Balmaseda A, Harris E (2015) Lower Low-Density Lipoprotein Cholesterol Levels Are Associated with Severe Dengue Outcome. *PLoS neglected tropical diseases* 9: e0003904

Brault AC, Domi A, McDonald EM, Talmi-Frank D, McCurley N, Basu R, Robinson HL, Hellerstein M, Duggal NK, Bowen RA *et al* (2017) A Zika Vaccine Targeting NS1 Protein Protects Immunocompetent Adult Mice in a Lethal Challenge Model. *Sci Rep* 7: 14769

Brown PH, Schuck P (2006) Macromolecular size-and-shape distributions by sedimentation velocity analytical ultracentrifugation. *Biophysical journal* 90: 4651-4661

Camont L, Chapman MJ, Kontush A (2011) Biological activities of HDL subpopulations and their relevance to cardiovascular disease. *Trends Mol Med* 17: 594-603

Chen J, Ng MM, Chu JJ (2015) Activation of TLR2 and TLR6 by Dengue NS1 Protein and Its Implications in the Immunopathogenesis of Dengue Virus Infection. *PLoS pathogens* 11: e1005053

Chung KM, Liszewski MK, Nybakken G, Davis AE, Townsend RR, Fremont DH, Atkinson JP, Diamond MS (2006) West Nile virus nonstructural protein NS1 inhibits complement activation by binding the regulatory protein factor H. *Proc Natl Acad Sci U S A* 103: 19111-19116

Coelho DR, Carneiro PH, Mendes-Monteiro L, Conde JN, Andrade I, Cao T, Allonso D, White-Dibiasio M, Kuhn RJ, Mohana-Borges R (2021) ApoA1 neutralizes pro-inflammatory effects of Dengue virus NS1 protein and modulates the viral immune evasion. *J Virol*

Conde JN, da Silva EM, Allonso D, Coelho DR, Andrade IDS, de Medeiros LN, Menezes JL, Barbosa AS, Mohana-Borges R (2016) Inhibition of the Membrane Attack Complex by Dengue Virus NS1 through Interaction with Vitronectin and Terminal Complement Proteins. *Journal of virology* 90: 9570-9581

Dewi BE, Takasaki T, Kurane I (2004) In vitro assessment of human endothelial cell permeability: effects of inflammatory cytokines and dengue virus infection. *Journal of virological methods* 121: 171-180

Espinosa DA, Beatty PR, Reiner GL, Sivick KE, Hix Glickman L, Dubensky TW, Jr., Harris E (2019) Cyclic Dinucleotide-Adjuvanted Dengue Virus Nonstructural Protein 1 Induces Protective Antibody and T Cell Responses. *J Immunol* 202: 1153-1162

Falconar AK (2007) Antibody responses are generated to immunodominant ELK/KLE-type motifs on the nonstructural-1 glycoprotein during live dengue virus infections in mice and humans: implications for diagnosis, pathogenesis, and vaccine design. *Clin Vaccine Immunol* 14: 493-504

Feingold KR, Grunfeld C (2000) The Effect of Inflammation and Infection on Lipids and Lipoproteins. In: *Endotext*, Feingold K.R., Anawalt B., Boyce A., Chrousos G., Dungan K., Grossman A., Hershman J.M., Kaltsas G., Koch C., Kopp P. *et al* (eds.)South Dartmouth (MA)

Filou S, Lhomme M, Karavia EA, Kalogeropoulou C, Theodoropoulos V, Zvintzou E, Sakellaropoulos GC, Petropoulou PI, Constantinou C, Kontush A *et al* (2016) Distinct Roles of Apolipoproteins A1 and E in the Modulation of High-Density Lipoprotein Composition and Function. *Biochemistry* 55: 3752-3762

Fink J, Gu F, Vasudevan SG (2006) Role of T cells, cytokines and antibody in dengue fever and dengue haemorrhagic fever. *Rev Med Virol* 16: 263-275

Flamand M, Chevalier M, Henchal E, Girard M, Deubel V (1995) Purification and renaturation of Japanese encephalitis virus nonstructural glycoprotein NS1 overproduced by insect cells. *Protein Expr Purif* 6: 519-527

Flamand M, Megret F, Mathieu M, Lepault J, Rey FA, Deubel V (1999) Dengue virus type 1 nonstructural glycoprotein NS1 is secreted from mammalian cells as a soluble hexamer in a glycosylation-dependent fashion. *Journal of virology* 73: 6104-6110

676 Flamand M, Salmon J, Rey FA, Gutsche I, Ermonval M, Kayal S, 2009. Nonstructural protein
677 NS1 as a novel therapeutic target against flaviviruses: Use of inhibiting molecules interfering
678 with NS1 maturation or biological activity, in: Pasteur I. (Ed.).

679 Glasner DR, Puerta-Guardo H, Beatty PR, Harris E (2018) The Good, the Bad, and the
680 Shocking: The Multiple Roles of Dengue Virus Nonstructural Protein 1 in Protection and
681 Pathogenesis. *Annu Rev Virol* 5: 227-253

682 Gogonea V (2015) Structural Insights into High Density Lipoprotein: Old Models and New
683 Facts. *Front Pharmacol* 6: 318

684 Green S, Rothman A (2006) Immunopathological mechanisms in dengue and dengue
685 hemorrhagic fever. *Curr Opin Infect Dis* 19: 429-436

686 Gutsche I, Coulibaly F, Voss JE, Salmon J, d'Alayer J, Ermonval M, Larquet E, Charneau P,
687 Krey T, Megret F *et al* (2011) Secreted dengue virus nonstructural protein NS1 is an atypical
688 barrel-shaped high-density lipoprotein. *Proceedings of the National Academy of Sciences of*
689 *the United States of America* 108: 8003-8008

690 Halsey ES, Williams M, Laguna-Torres VA, Vilcarromero S, Ocana V, Kochel TJ, Marks
691 MA (2014) Occurrence and correlates of symptom persistence following acute dengue fever
692 in Peru. *The American journal of tropical medicine and hygiene* 90: 449-456

693 Huang J, Liang W, Chen S, Zhu Y, Chen H, Mok CKP, Zhou Y (2018) Serum Cytokine
694 Profiles in Patients with Dengue Fever at the Acute Infection Phase. *Dis Markers* 2018:
695 8403937

696 Jacobs MG, Robinson PJ, Bletchly C, Mackenzie JM, Young PR (2000) Dengue virus
697 nonstructural protein 1 is expressed in a glycosyl-phosphatidylinositol-linked form that is
698 capable of signal transduction. *Faseb J* 14: 1603-1610

699 Jayaraman S, Haupt C, Gursky O (2015) Thermal transitions in serum amyloid A in solution
700 and on the lipid: implications for structure and stability of acute-phase HDL. *Journal of lipid*
701 *research* 56: 1531-1542

702 Jayathilaka D, Gomes L, Jeewandara C, Jayarathna GSB, Herath D, Perera PA, Fernando S,
703 Wijewickrama A, Hardman CS, Ogg GS *et al* (2018) Role of NS1 antibodies in the
704 pathogenesis of acute secondary dengue infection. *Nat Commun* 9: 5242

Kopecky C, Michlits G, Saemann MD, Weichhart T (2017) Pro- versus Anti-inflammatory Actions of HDLs in Innate Immunity. *Cell Metab* 26: 2-3

Kurosu T, Chaichana P, Yamate M, Anantapreecha S, Ikuta K (2007) Secreted complement regulatory protein clusterin interacts with dengue virus nonstructural protein 1. *Biochem Biophys Res Commun* 362: 1051-1056

Lauer ME, Graff-Meyer A, Rufer AC, Maugeais C, von der Mark E, Matile H, D'Arcy B, Magg C, Ringler P, Muller SA *et al* (2016) Cholesteryl ester transfer between lipoproteins does not require a ternary tunnel complex with CETP. *Journal of structural biology* 194: 191-198

Lee YH, Leong WY, Wilder-Smith A (2016) Markers of dengue severity: a systematic review of cytokines and chemokines. *The Journal of general virology* 97: 3103-3119

Libraty DH, Young PR, Pickering D, Endy TP, Kalayanarooj S, Green S, Vaughn DW, Nisalak A, Ennis FA, Rothman AL (2002) High circulating levels of the dengue virus nonstructural protein NS1 early in dengue illness correlate with the development of dengue hemorrhagic fever. *J Infect Dis* 186: 1165-1168

Lima WG, Souza NA, Fernandes SOA, Cardoso VN, Godoi IP (2019) Serum lipid profile as a predictor of dengue severity: A systematic review and meta-analysis. *Reviews in medical virology* 29: e2056

Lin CF, Wan SW, Cheng HJ, Lei HY, Lin YS (2006) Autoimmune pathogenesis in dengue virus infection. *Viral Immunol* 19: 127-132

Lin SW, Chuang YC, Lin YS, Lei HY, Liu HS, Yeh TM (2011) Dengue virus nonstructural protein NS1 binds to prothrombin/thrombin and inhibits prothrombin activation. *J Infect*

Lin SW, Chuang YC, Lin YS, Lei HY, Liu HS, Yeh TM (2012) Dengue virus nonstructural protein NS1 binds to prothrombin/thrombin and inhibits prothrombin activation. *The Journal of infection* 64: 325-334

Lindenbach BD, Rice CM (1997) *trans*-Complementation of yellow fever virus NS1 reveals a role in early RNA replication. *J Virol* 71: 9608-9617

Lindenbach BD, Rice CM (2003) Molecular biology of flaviviruses. *Adv Virus Res* 59: 23-61

Luengas LL, Tiga DC, Herrera VM, Villar-Centeno LA (2015) Characterization of the health condition of people convalescing from a dengue episode. *Biomedica* 36: 89-97

735 Marais AD (2019) Apolipoprotein E in lipoprotein metabolism, health and cardiovascular
736 disease. *Pathology* 51: 165-176

737 Marin-Palma D, Sirois CM, Urcuqui-Inchima S, Hernandez JC (2019) Inflammatory status
738 and severity of disease in dengue patients are associated with lipoprotein alterations. *PLoS*
739 *One* 14: e0214245

740 Marsche G, Saemann MD, Heinemann A, Holzer M (2013) Inflammation alters HDL
741 composition and function: implications for HDL-raising therapies. *Pharmacology &*
742 *therapeutics* 137: 341-351

743 Modhiran N, Watterson D, Blumenthal A, Baxter AG, Young PR, Stacey KJ (2017) Dengue
744 virus NS1 protein activates immune cells via TLR4 but not TLR2 or TLR6. *Immunol Cell*
745 *Biol* 95: 491-495

746 Modhiran N, Watterson D, Muller DA, Panetta AK, Sester DP, Liu L, Hume DA, Stacey KJ,
747 Young PR (2015) Dengue virus NS1 protein activates cells via Toll-like receptor 4 and
748 disrupts endothelial cell monolayer integrity. *Sci Transl Med* 7: 304ra142

749 Murch O, Collin M, Hinds CJ, Thiemermann C (2007) Lipoproteins in inflammation and
750 sepsis. I. Basic science. *Intensive Care Med* 33: 13-24

751 Pang T, Cardosa MJ, Guzman MG (2007) Of cascades and perfect storms: the
752 immunopathogenesis of dengue haemorrhagic fever-dengue shock syndrome (DHF/DSS).
753 *Immunol Cell Biol* 85: 43-45

754 Prufer N, Kleuser B, van der Giet M (2015) The role of serum amyloid A and sphingosine-1-
755 phosphate on high-density lipoprotein functionality. *Biological chemistry* 396: 573-583

756 Puerta-Guardo H, Glasner DR, Espinosa DA, Biering SB, Patana M, Ratnasiri K, Wang C,
757 Beatty PR, Harris E (2019) Flavivirus NS1 Triggers Tissue-Specific Vascular Endothelial
758 Dysfunction Reflecting Disease Tropism. *Cell Rep* 26: 1598-1613 e1598

759 Puerta-Guardo H, Glasner DR, Harris E (2016) Dengue Virus NS1 Disrupts the Endothelial
760 Glycocalyx, Leading to Hyperpermeability. *PLoS pathogens* 12: e1005738

761 Ramasamy I (2014) Recent advances in physiological lipoprotein metabolism. *Clin Chem*
762 *Lab Med* 52: 1695-1727

763 Rastogi M, Sharma N, Singh SK (2016) Flavivirus NS1: a multifaceted enigmatic viral
764 protein. *Virology journal* 13: 131

765 Rathakrishnan A, Wang SM, Hu Y, Khan AM, Ponnampalavanar S, Lum LC, Manikam R,
766 Sekaran SD (2012) Cytokine expression profile of dengue patients at different phases of
767 illness. *PLoS One* 7: e52215

768 Ronsein GE, Vaisar T (2019) Deepening our understanding of HDL proteome. *Expert Rev*
769 *Proteomics* 16: 749-760

770 Saemann MD, Poglitsch M, Kopecky C, Haidinger M, Horl WH, Weichhart T (2010) The
771 versatility of HDL: a crucial anti-inflammatory regulator. *European journal of clinical*
772 *investigation* 40: 1131-1143

773 Scheres SH (2012) RELION: implementation of a Bayesian approach to cryo-EM structure
774 determination. *Journal of structural biology* 180: 519-530

775 Schlesinger JJ, Brandriss MW, Walsh EE (1985) Protection against 17 D yellow fever
776 encephalitis in mice by passive transfer of monoclonal antibodies to the nonstructural
777 glycoprotein gp48 and by active immunization with gp48. *J Immunol* 135: 2805-2809

778 Schlesinger JJ, Brandriss MW, Walsh EE (1987) Protection of mice against dengue 2 virus
779 encephalitis by immunization with the dengue 2 virus nonstructural glycoprotein NS1. *J Gen*
780 *Virol* 68: 853-857

781 Shao B, Heinecke JW (2018) Quantifying HDL proteins by mass spectrometry: how many
782 proteins are there and what are their functions? *Expert Rev Proteomics* 15: 31-40

783 Srikiatkhachorn A, Mathew A, Rothman AL (2017) Immune-mediated cytokine storm and its
784 role in severe dengue. *Semin Immunopathol* 39: 563-574

785 Su X, Peng D (2020) The exchangeable apolipoproteins in lipid metabolism and obesity. *Clin*
786 *Chim Acta* 503: 128-135

787 Sun DS, King CC, Huang HS, Shih YL, Lee CC, Tsai WJ, Yu CC, Chang HH (2007)
788 Antiplatelet autoantibodies elicited by dengue virus non-structural protein 1 cause
789 thrombocytopenia and mortality in mice. *J Thromb Haemost* 5: 2291-2299

790 Suvarna JC, Rane PP (2009) Serum lipid profile: a predictor of clinical outcome in dengue
791 infection. *Trop Med Int Health* 14: 576-585

792 Teixeira LAS, Nogueira F, Nascentes GAN (2017) Prospective study of patients with
793 persistent symptoms of dengue in Brazil. *Rev Inst Med Trop Sao Paulo* 59: e65

794 Tiga-Loza DC, Martinez-Vega RA, Undurraga EA, Tschampl CA, Shepard DS, Ramos-
795 Castaneda J (2020) Persistence of symptoms in dengue patients: a clinical cohort study.
796 *Transactions of the Royal Society of Tropical Medicine and Hygiene*

797 Tramontini Gomes de Sousa Cardozo F, Baimukanova G, Lanteri MC, Keating SM, Moraes
798 Ferreira F, Heitman J, Pannuti CS, Pati S, Romano CM, Cerdeira Sabino E (2017) Serum
799 from dengue virus-infected patients with and without plasma leakage differentially affects
800 endothelial cells barrier function in vitro. *PLoS One* 12: e0178820

801 Valanti EK, Dalakoura-Karagkouni K, Sanoudou D (2018) Current and Emerging
802 Reconstituted HDL-apoA-I and HDL-apoE Approaches to Treat Atherosclerosis. *J Pers Med*
803 8

804 van Gorp EC, Suharti C, Mairuhu AT, Dolmans WM, van Der Ven J, Demacker PN, van Der
805 Meer JW (2002) Changes in the plasma lipid profile as a potential predictor of clinical
806 outcome in dengue hemorrhagic fever. *Clin Infect Dis* 34: 1150-1153

807 Velazquez-Muriel JA, Sorzano CO, Scheres SH, Carazo JM (2005) SPI-EM: towards a tool
808 for predicting CATH superfamilies in 3D-EM maps. *J Mol Biol* 345: 759-771

809 Wan SW, Yang YW, Chu YT, Lin CF, Chang CP, Yeh TM, Anderson R, Lin YS (2016) Anti-
810 dengue virus nonstructural protein 1 antibodies contribute to platelet phagocytosis by
811 macrophages. *Thrombosis and Haemostasis* 115: 646-656

812 Watterson D, Modhiran N, Young PR (2016) The many faces of the flavivirus NS1 protein
813 offer a multitude of options for inhibitor design. *Antiviral research* 130: 7-18

814 Wilder-Smith A, Ooi EE, Horstick O, Wills B (2019) Dengue. *Lancet* 393: 350-363

815 Winkler G, Maxwell SE, Ruemmler C, Stollar V (1989) Newly synthesized dengue-2 virus
816 nonstructural protein NS1 is a soluble protein but becomes partially hydrophobic and
817 membrane-associated after dimerization. *Virology* 171: 302-305

818 Wu A, Hinds CJ, Thiemermann C (2004) High-density lipoproteins in sepsis and septic shock:
819 metabolism, actions, and therapeutic applications. *Shock* 21: 210-221

820 Yacoub S, Mongkolsapaya J, Screaton G (2013) The pathogenesis of dengue. *Current opinion*
821 *in infectious diseases* 26: 284-289

822 Yacoub S, Mongkolsapaya J, Screaton G (2016) Recent advances in understanding dengue.
823 *F1000Res* 5

824 Zhang L, Tong H, Garewal M, Ren G (2013) Optimized negative-staining electron
825 microscopy for lipoprotein studies. *Biochimica et biophysica acta* 1830: 2150-2159

826

FIGURE LEGENDS

Fig. 1: DENV NS1 binds to human high-density and low-density lipoproteins

(A) Size exclusion chromatography profile of NS1 pull-down experiments showing a clear shift after incubation in complete or heat-inactivated human serum (solid and dotted black lines, respectively) from the same healthy donor compared to the NS1 protein alone (blue line). NS1 protein interaction partners were identified by SDS-PAGE and N-terminal sequencing as the Apolipoprotein B scaffold of the low-density lipoproteins (LDL) in the first SEC elution peak, and the ApoA-I protein scaffold of the high-density lipoproteins (HDL) in the second elution peak.

(B) Biolayer interferometry (BLI) profiles corresponding to the binding of NS1 at various concentrations respective to human HDL (left panel) and human LDL (central panel) particles. The concentration-dependence of the steady-state signal corresponding to the binding of NS1 to HDL (black dots) and LDL (white dots) is shown on the right-hand side panel. The measurements were replicated at least three times using novel biosensors and samples. Data points and error bars correspond to the mean ± SD.

(C) Typical sedimentation coefficient distribution of NS1 or human HDL alone or pre-incubated together (mixture of NS1 and HDL at a 1:1 or 5:1 mass ratio) monitored using an interferometric detector. Peaks were integrated for all the detectors (interference and absorbance at 280nm). The calculated stoichiometries are indicated for each peak. Solutions were equilibrated at 20°C for 2h before sedimentation velocity analysis.

Fig. 2: Analysis of NS1-HDL complexes by electron microscopy reveals the presence of NS1 dimers on the surface of HDL particles

(A, B) Electron microscopy observations from left to right: a representative image, followed by the three most representative classes of (A) purified HDL particles and (B) NS1-HDL complexes. White bar: 50 nm, Black bar: 20 nm.

(C) Fitting of the NS1 3D structure of the dimeric form into the most abundant class of NS1-HDL complexes, suggesting a collapse of the NS1 hexamer into hydrophobic dimeric blocks that float and anchor into the HDL lipid phase.

(D) Differential scanning calorimetry (DSC) of NS1 alone (blue line) or of an NS1-HDL mixture at a 2:1 molar ratio (orange). Of note, the HDL particles alone did not generate any signal in the temperature range tested.

(E) Binding inhibition of hexameric NS1 to HDL with anti-ApoA-I polyclonal antibodies (anti-ApoA-I Ab) measured by BLI.

Fig. 3: The NS1-HDL lipoprotein complex triggers pro-inflammatory signals in human primary macrophages

(A-D) Human primary macrophages were incubated for 24h with the different potential effectors (NS1, HDL, mix NS1-HDL) or with control suspensions (PBS buffer, LPS, mix LPS-HDL). LPS stimulation was used as a positive control in the presence or absence of HDL and provided values consistent between experiments. Phosphate buffer used in the SEC purification step was used as a negative control. Cell culture supernatants were clarified and tested with a Luminex assay to quantify the amount of (A) TNF-α, (B) Il-6, (C) Il-1ß and (D) Il-10 released in the extracellular medium. Data reported on the graphs correspond to biological replicates of macrophages isolated from four blood donors (n=9 for TNF-α, Il-6

874 and Il-1ß, n=5 for Il-10). Data represent mean +/- SEM. A Mann-Whitney test was used to
875 assess the statistical significance of differences observed between mean cytokine levels in
876 different cell culture supernatants. Not significant: ns, * $p < 0.05$, *** $p < 0.001$.
877
878 **Fig. 4. Different biological and virological parameters measured in human plasma**.
879 (A-H) DENV-infected hospitalized patients from the Kampong Cham Referral Hospital,
880 Cambodia, presented either dengue with warning signs or severe dengue. Two blood samples
881 were recovered for each patient on the day of hospital admission and during a follow-up visit
882 that occurred before discharge from the hospital (on average 4 days apart). (A) Number of
883 patient samples tested over the hospitalization period for their levels of (B) NS1, (C) NS1-
884 ApoA-I, (D) NS1-ApoE and (E) NS1-ApoB complexes in addition to (F) total cholesterol,
885 (G) HDL-cholesterol and (H) triglycerides. NS1-ApoA-I and NS1-ApoB complexes are
886 representative of NS1-HDL and NS1-LDL complex species, respectively, while the NS1-
887 ApoE-positive complexes remain to be fully characterized. Errors bars indicate SEM.
888 (I) Purified NS1 from different flaviviruses (yellow fever, YF; ZIKA; West Nile, WN;
889 Japanese encephalitis, JE; The Native Antigen Company) were spiked in normal human
890 plasma and NS1-ApoA-I complexes further detected by ELISA. Data represent the mean
891 values of two technical replicates.

892 **EXPANDED VIEW FIGURE LEGENDS**

893

894 **Fig. EV1: The secreted form of DENV-2 NS1 binds to bovine HDL and LDL.**

895 (A-C) The NS1 protein was expressed in *drosophila* S2 cells cultured either in InsectXpress
896 protein-free medium (Lonza) supplemented with 5% complete fetal bovine serum (FBS) or
897 without FBS. NS1 was purified on a Streptactin affinity column before analysis in a size
898 exclusion column (superdex 200 16/60).

899 (A) Typical chromatograms obtained with purified secreted DENV-2 NS1 (blue line) and
900 DENV-2 NS1 bovine complexes (red line) are shown.

901 (B) Denaturing SDS-PAGE analysis of 1 fraction every 4 mL from 38 to 75 mL elution
902 volume. Molecular weights of protein standards (Std) are expressed in kDa. Proteins were
903 detected by UV (Stain-free, Biorad). The three major protein bands identified by mass-
904 spectrometry are bovine ApoB (>250 kDa), DENV-2 NS1 (~50 kDa), and bovine ApoA-I
905 (~25 kDa).

906 (C) Negative-stain electron micrographs of purified hexameric NS1 alone (left panel) or
907 purified as a complex with ApoA-I (NS1-HDL, central panel) or with ApoB (NS1-LDL, right
908 panel). Bar: 100 nm. Data are derived from at least two independent experiments.

909

910 **Fig. EV2: Co-immunoprecipitation of native NS1 and apolipoproteins from DENV-**
911 **infected cells cultured in media supplemented with bovine or human serum.**

912 (A-B) Vero cells infected with DENV (strain 16681) at an MOI of 1 or uninfected were
913 cultured for 3 days in media supplemented with 10% FBS or 10% human serum. Supernatants
914 were clarified by centrifugation and immunoprecipitated with (A) anti-NS1 MAb 17A12 or
915 anti-ApoA-I PAbs or (B) with anti-NS1 MAb 17A12 or anti-ApoE PAbs. The resulting
916 products were separated by SDS-PAGE on stain-free gels, submitted to UV light and

visualized in a gel imager (G-Box, Syngene) (A,B), or transferred onto a PVDF membrane treated with biotinylated anti-ApoE PAb and streptavidin-HRP (B). Data shown are representative of two technical replicates.

Fig. EV3: Dose-dependent binding of NS1 to HDL particles monitored by biolayer interferometry.

(A-C) Biolayer interferometry (BLI) profiles corresponding to the binding of NS1 at various concentrations respective to human HDL particles. Data from NS1 binding to (A) HDL loaded biosensors, (B) antibody activated biosensors and (C) the corresponding subtraction. Data was colored according to the NS1 concentration as 800 nM in Magenta, 400 nM in violet, 200 nM in blue, 100 nM in sky blue, 50 nM in green, 25 nM in apple green, 12.5 nM in orange and 6.25 nM in red.

Fig. EV4: Electron microscopy analysis of NS1-HDL complexes.

(A, B) Classes of NS1 and NS1-HDL purified species from negative-stain electron microscopy (EM) images. NS1 and NS1-HDL were purified as described in Material and Methods. The corresponding protein fractions were recovered from size exclusion chromatography and analyzed by negative-stain EM. Automated acquisitions were performed using EPU software and images were acquired using a Falcon II direct detector. Images were CTF-corrected (phase flip) and sorted using the XMIP software 84. Sizes of squares are reported at the bottom right of each panel.

(C) Representative electron microscopy image of negatively-stained NS1-HDL complexes bound to Fab 17A12. NS1-HDL complexes were formed at a 1:1 molar ratio, purified by SEC and further incubated with Fab 17A12 at a molar ratio of 3 Fab:1 NS1-HDL complex. Samples were spotted on glow discharged grids and contrasted with 2% uranyl actetate. Images were

acquired on a Tecnai F20 microscope operated at 200kV using EPU software (Thermo-Fisher, USA) on a Falcon II camera, under low dose conditions. Bar: 20 nm. Image representative of at least four different fields.

Fig. EV5: Standard calibration curves.

(A-E) Detection of the DENV NS1 protein and NS1-ApoA-I, NS1-ApoB or NS1-ApoE complexes by sandwich ELISA**.** (A) Detection of the purified DENV NS1 has been described previously [11]. (B) NS1-ApoA-I, NS1-ApoB or NS1-ApoE complexes were formed in normal plasma spiked with purified NS1 at a known concentration. Capture of the NS1-ApoA-I, NS1-ApoB or NS1-ApoE complexes were carried out using an anti-NS1 monoclonal antibody (MAb17A12). The detection of immobilized complexes was performed with an anti-ApoA-I, anti-ApoB or anti-ApoE polyclonal antibody followed by a species-specific secondary antibody. The concentration of the NS1-ApoA-I, NS1-ApoB or NS1-ApoE complexes is reported on the basis of 100% NS1 bound to (C) HDL, (D) LDL or (E) ApoE-positive lipoprotein particles, respectively. Detection limits of the NS1, NS1-ApoA-I, NS1-ApoB or NS1-ApoE assays were set as twice the mean value of signals obtained with normal human plasma in the absence of NS1, which corresponded to 0.5, 17, 5 and 15 ng of an equivalent NS1 concentration per milliliter, respectively.

(F) Determination of the HDL molecular weight by mass photometry. Purified HDL were diluted at 5 µg/mL and deposited on the coverslip. Measurements were performed according to the procedure described in Wu and Piszczek (*Eur Biophys J,* **2021**, vol. 50: 403–409). The results show an average mass of 162kDa for the overall distribution.

Fig. 1

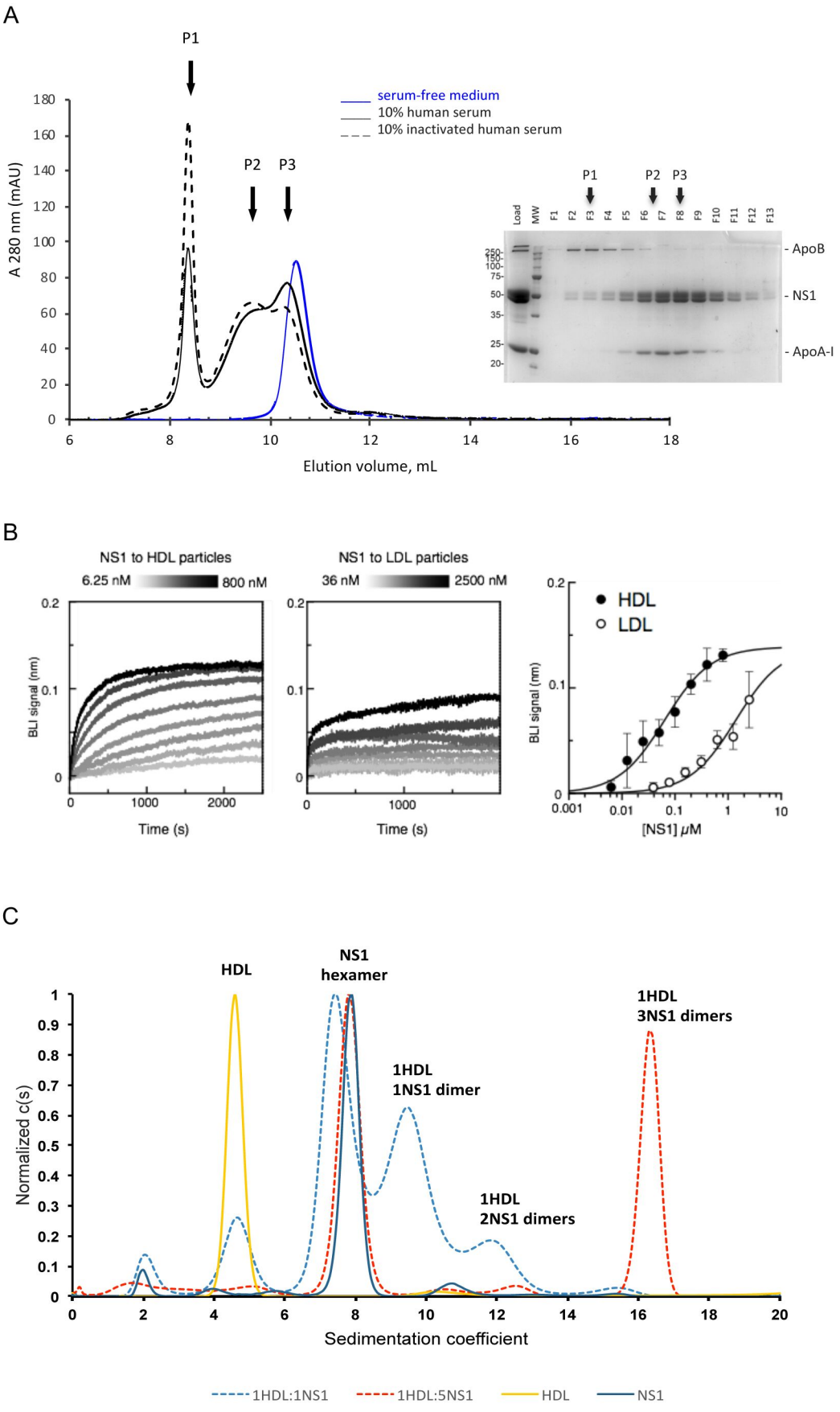
A
P1
P2
P3
serum-free medium
10% human serum
10% inactivated human serum
A 280 nm (mAU)
Elution volume, mL
Load
MW
F1
F2
F3
F4
F5
F6
F7
F8
F9
F10
F11
F12
F13
- ApoB
- NS1
- ApoA-I
B
NS1 to HDL particles
6.25 nM
800 nM
NS1 to LDL particles
36 nM
2500 nM
BLI signal (nm)
Time (s)
HDL
LDL
[NS1] μM
C
HDL
NS1 hexamer
1HDL 1NS1 dimer
1HDL 2NS1 dimers
1HDL 3NS1 dimers
Normalized c(s)
Sedimentation coefficient
1HDL:1NS1
1HDL:5NS1
HDL
NS1

Fig. 2

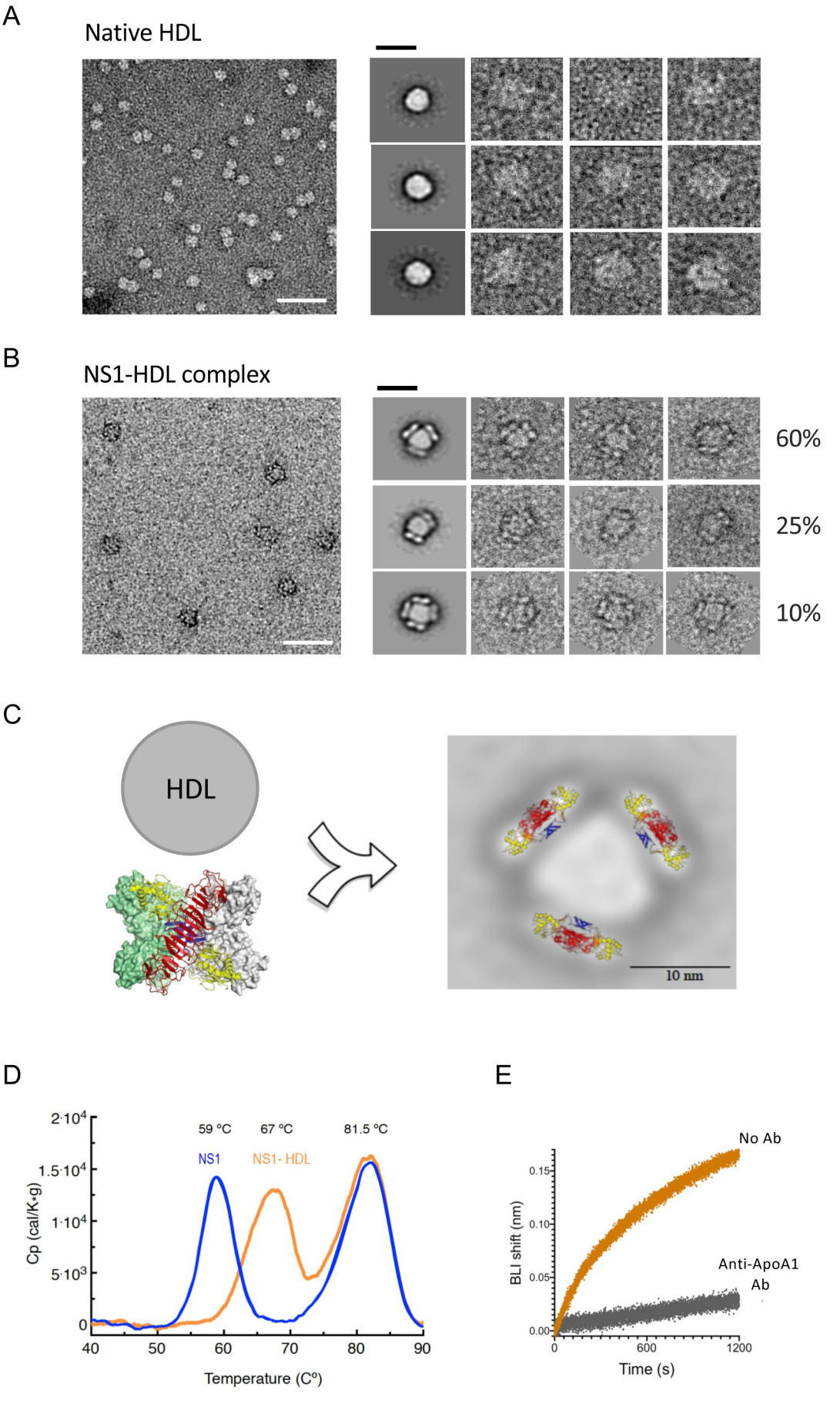
A
Native HDL
B
NS1-HDL complex
60%
25%
10%
C
HDL
10 nm
D
59 °C
67 °C
81.5 °C
NS1
NS1- HDL
Cp (cal/K·g)
Temperature (C°)
E
No Ab
Anti-ApoA1 Ab
BLI shift (nm)
Time (s)

Fig. 3

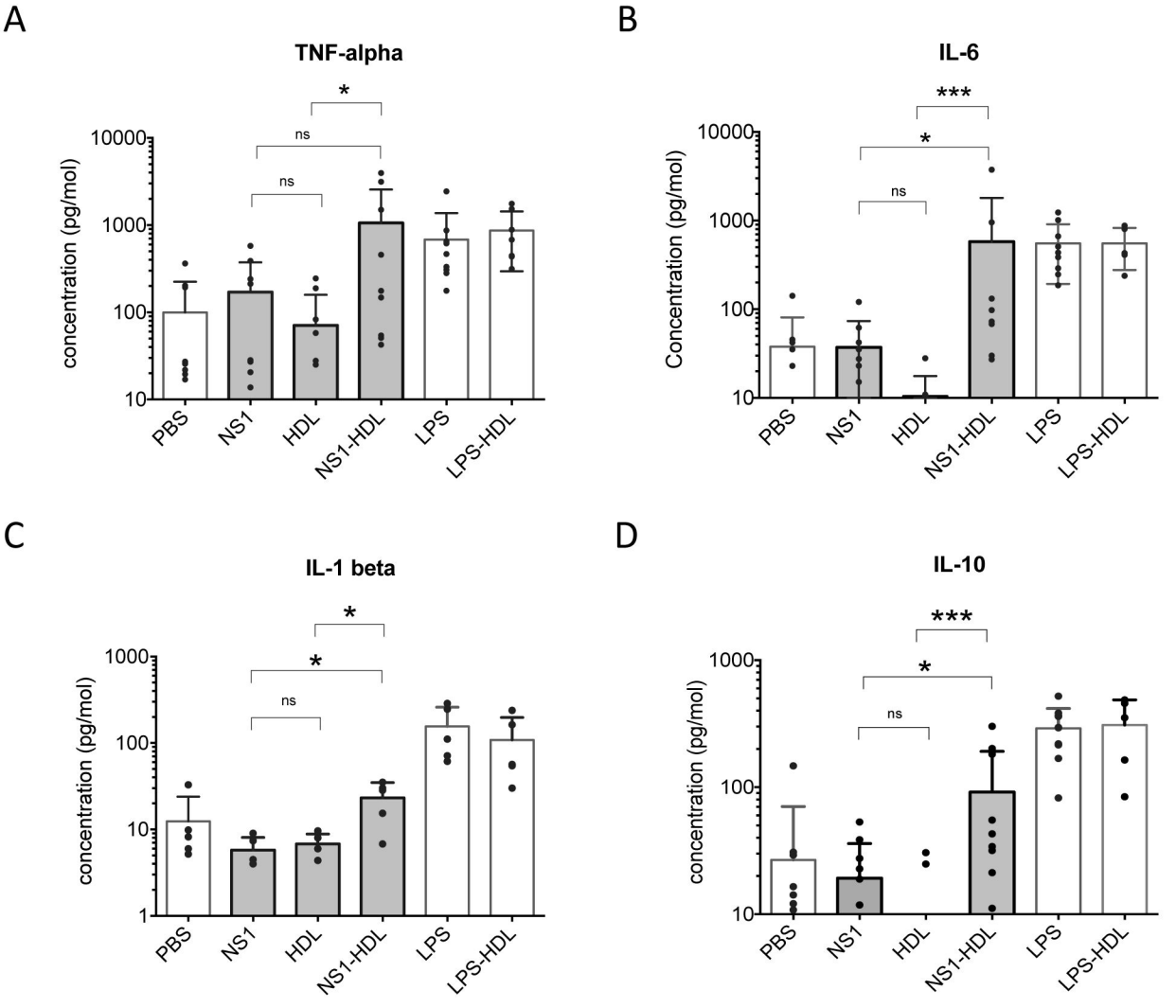
A
TNF-alpha
concentration (pg/mol)
10000
1000
100
10
*
ns
ns
PBS
NS1
HDL
NS1-HDL
LPS
LPS-HDL
B
IL-6
Concentration (pg/mol)
10000
1000
100
10
***
*
ns
PBS
NS1
HDL
NS1-HDL
LPS
LPS-HDL
C
IL-1 beta
concentration (pg/mol)
1000
100
10
1
*
*
ns
PBS
NS1
HDL
NS1-HDL
LPS
LPS-HDL
D
IL-10
concentration (pg/mol)
1000
100
10
***
*
ns
PBS
NS1
HDL
NS1-HDL
LPS
LPS-HDL

Fig. 4

A

Nb of days post-onset of fever		2	3	4	5	6	7	8	9	10
N= nb of patient samples	Panel B-C-D Panel F-G-H	5	6	11	21	11	18	13	12	5
	Panel E	9	5	7	7	4	3			

B

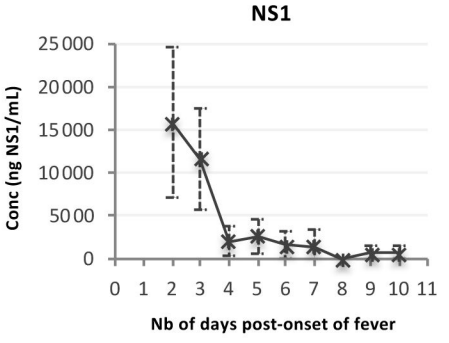

F

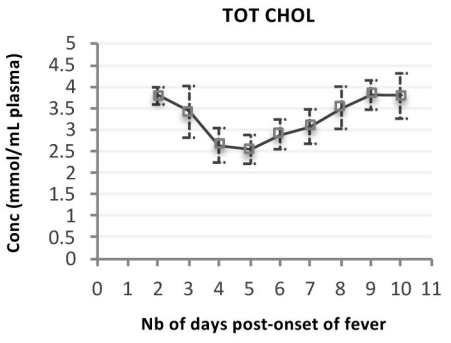

C

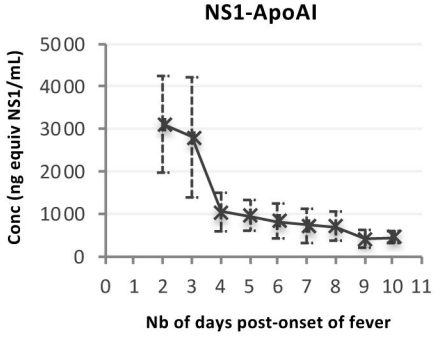

G

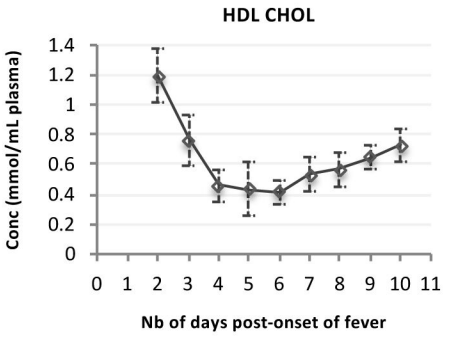

D

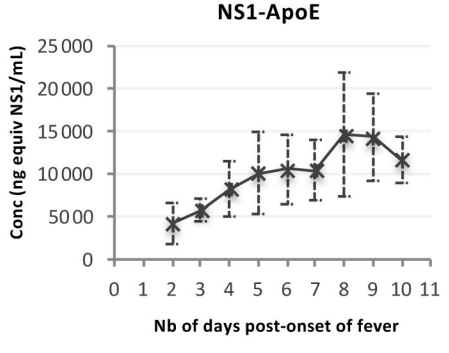

H

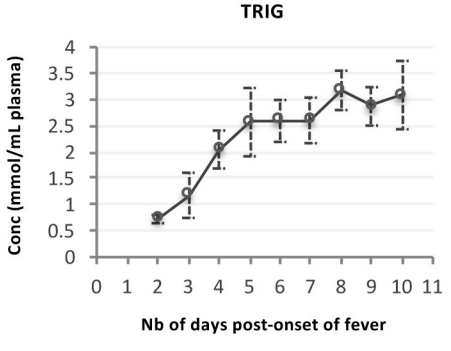

E

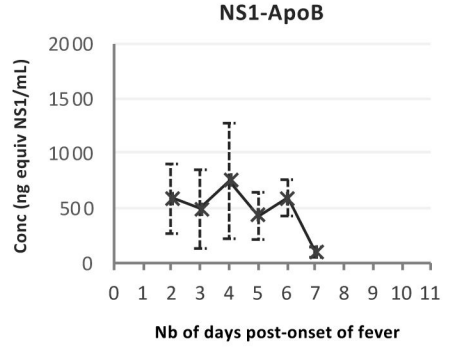

I

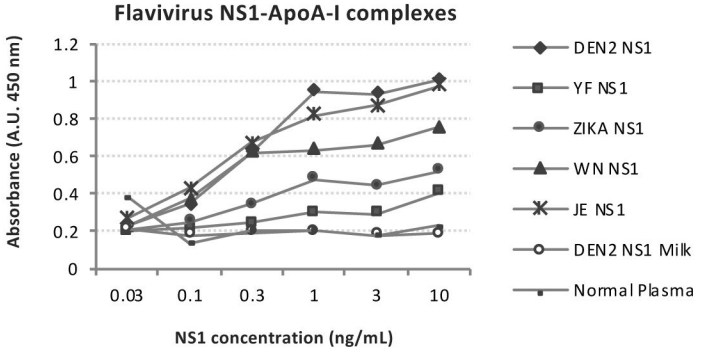

Fig. EV1

A

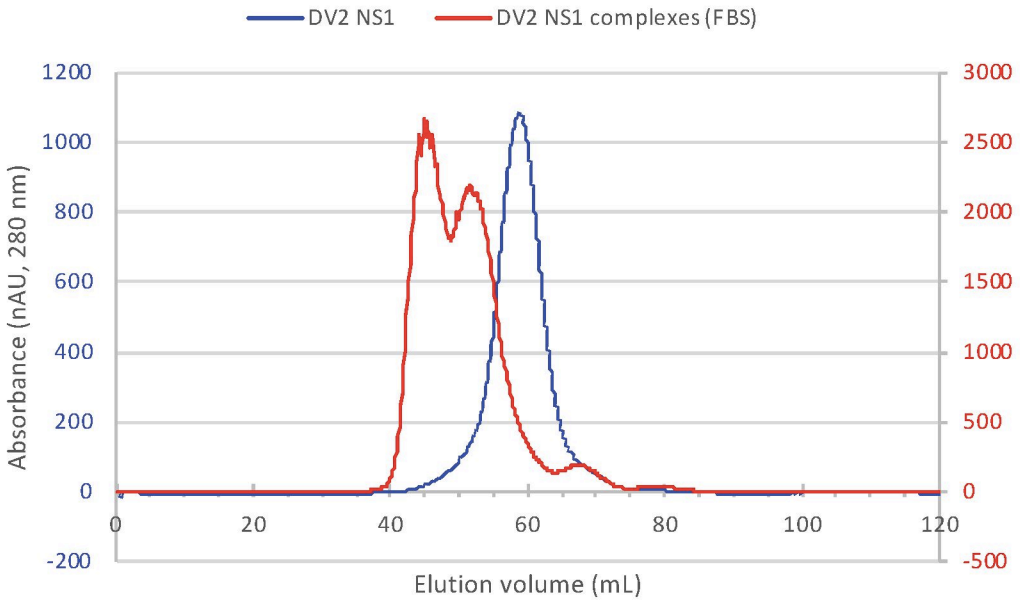
DV2 NS1
DV2 NS1 complexes (FBS)
Absorbance (nAU, 280 nm)
1200
1000
800
600
400
200
0
-200
3000
2500
2000
1500
1000
500
0
-500
0
20
40
60
80
100
120
Elution volume (mL)

B

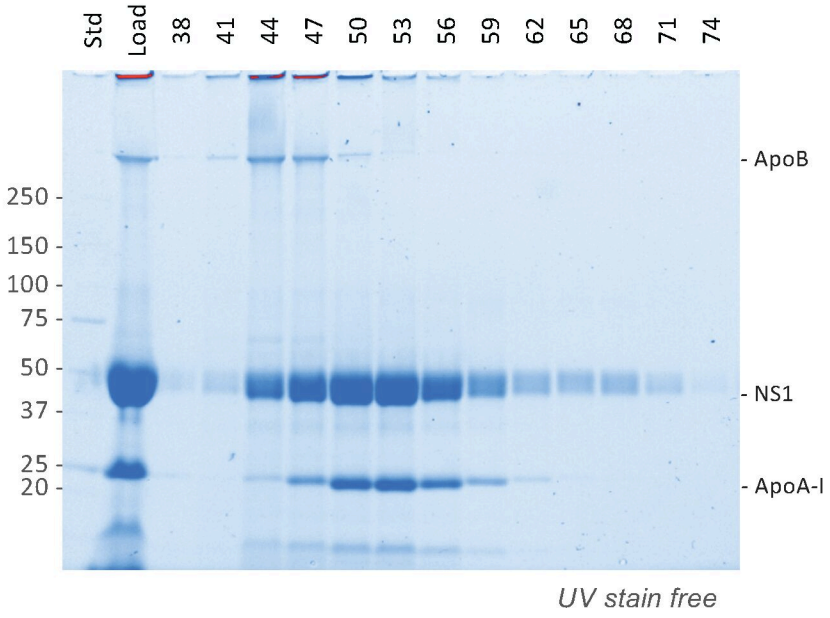
Std
Load
38
41
44
47
50
53
56
59
62
65
68
71
74
250
150
100
75
50
37
25
20
- ApoB
- NS1
- ApoA-I
UV stain free

C

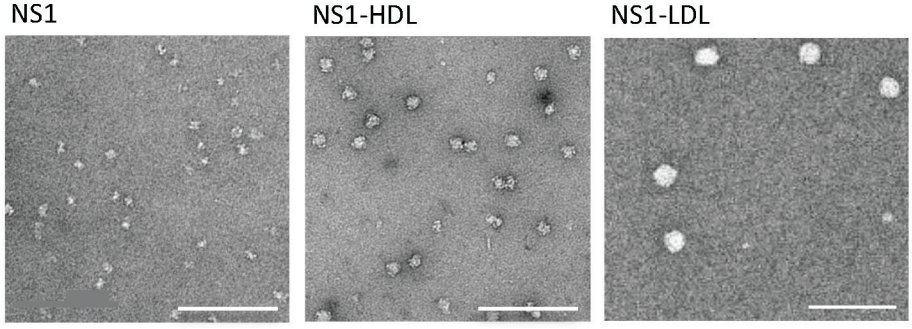
NS1
NS1-HDL
NS1-LDL

Fig. EV2

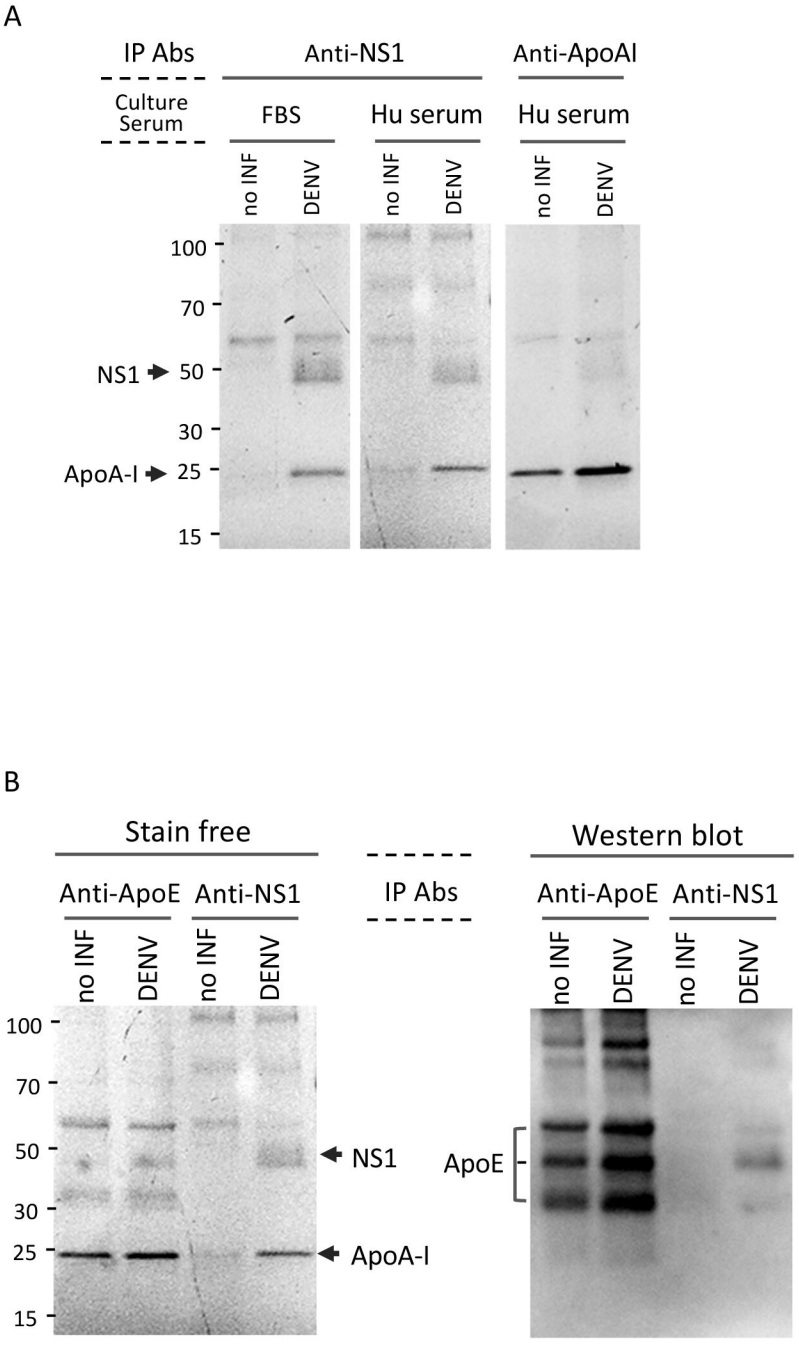
A
IP Abs
Anti-NS1
Anti-ApoAI
Culture Serum
FBS
Hu serum
Hu serum
no INF
DENV
no INF
DENV
no INF
DENV
100
70
NS1
50
30
ApoA-I
25
15
B
Stain free
Anti-ApoE
Anti-NS1
IP Abs
Western blot
Anti-ApoE
Anti-NS1
no INF
DENV
no INF
DENV
no INF
DENV
no INF
DENV
100
70
50
30
25
15
NS1
ApoA-I
ApoE

Fig. EV3

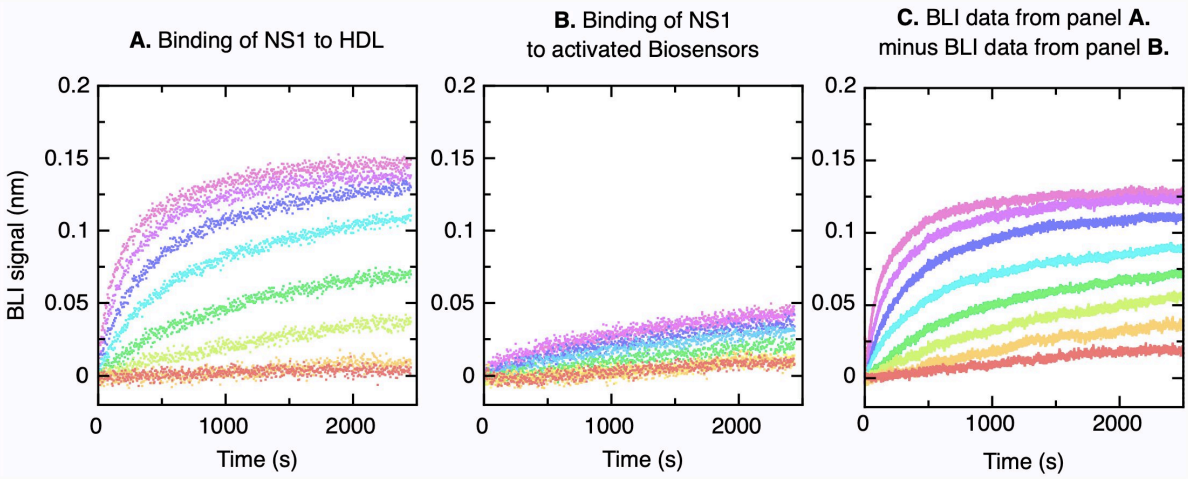
A. Binding of NS1 to HDL
B. Binding of NS1 to activated Biosensors
C. BLI data from panel A. minus BLI data from panel B.
BLI signal (nm)
0.2
0.15
0.1
0.05
0
0
1000
2000
Time (s)

Fig. EV4

A

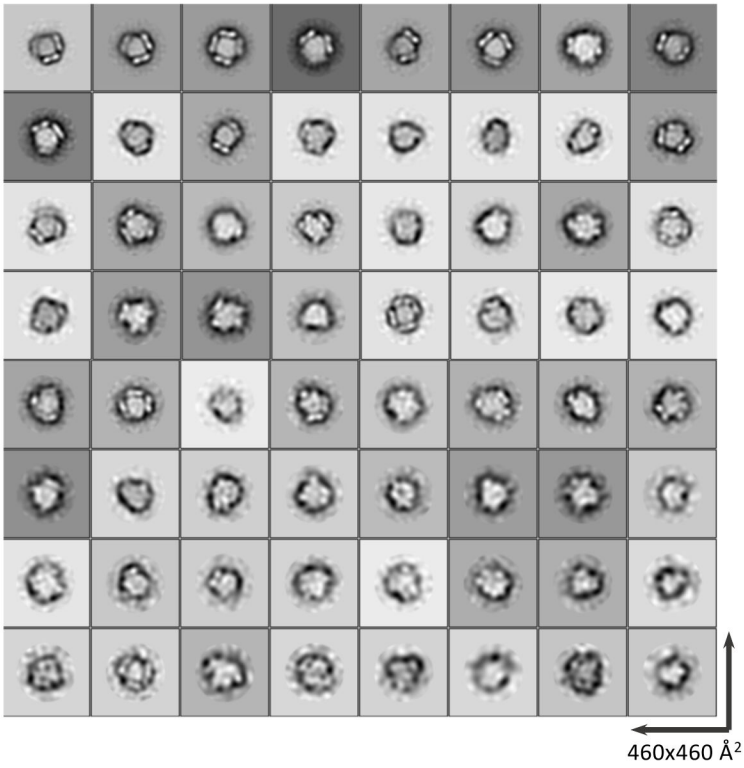

NS1-HDL

B

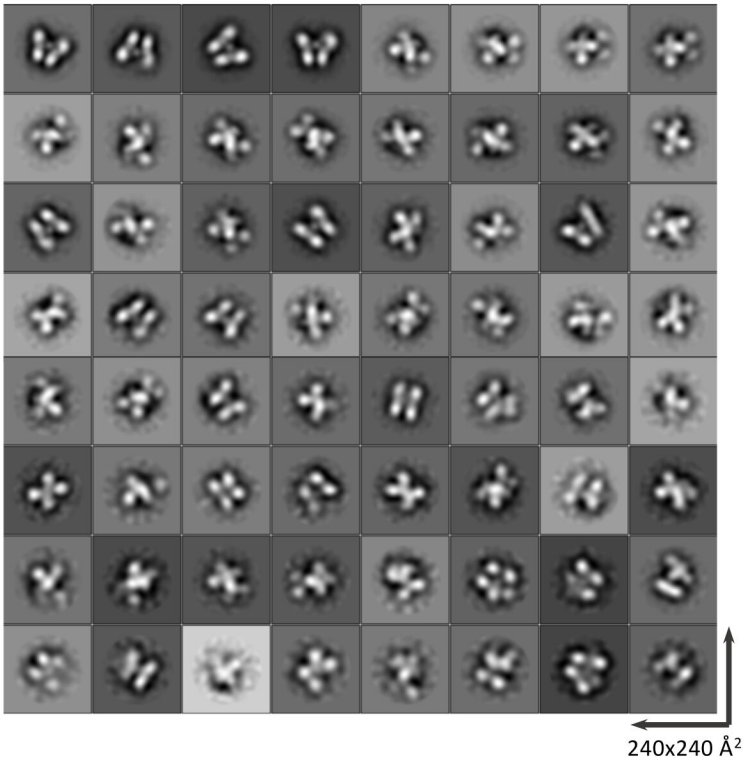

NS1

C

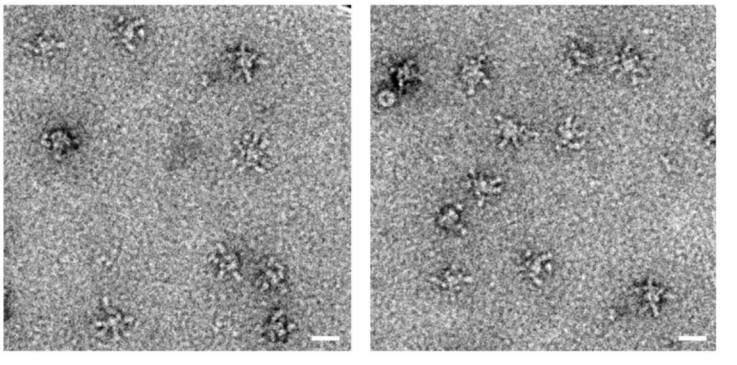

NS1-HDL-FAb 17A12

Fig. EV5

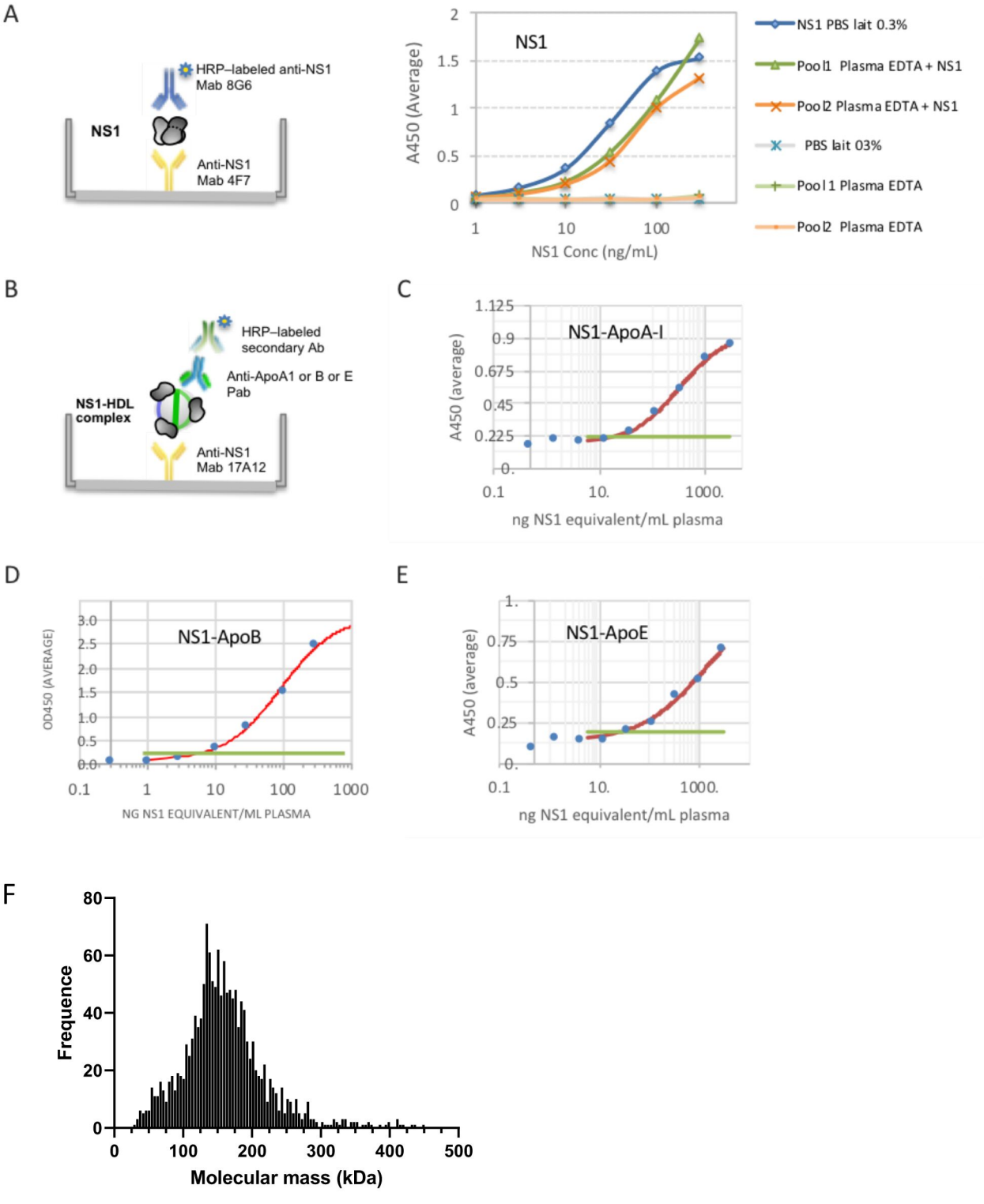
A
HRP–labeled anti-NS1 Mab 8G6
NS1
Anti-NS1 Mab 4F7
NS1
A450 (Average)
NS1 Conc (ng/mL)
NS1 PBS lait 0.3%
Pool1 Plasma EDTA + NS1
Pool2 Plasma EDTA + NS1
PBS lait 03%
Pool 1 Plasma EDTA
Pool2 Plasma EDTA
B
HRP–labeled secondary Ab
Anti-ApoA1 or B or E Pab
NS1-HDL complex
Anti-NS1 Mab 17A12
C
NS1-ApoA-I
A450 (average)
ng NS1 equivalent/mL plasma
D
NS1-ApoB
OD450 (AVERAGE)
NG NS1 EQUIVALENT/ML PLASMA
E
NS1-ApoE
A450 (average)
ng NS1 equivalent/mL plasma
F
Frequence
Molecular mass (kDa)